# PERFORMANCE INVESTIGATIONS ON DSP BASED PERMANENT MAGNET SYNCHRONOUS MOTOR DRIVE

## A DISSERTATION

*Submitted in partial fulfillment of the*
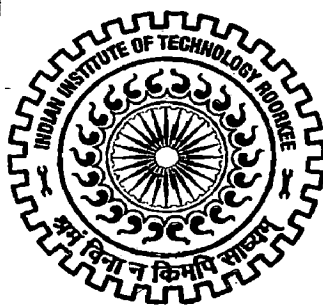*requirements for the award of the degree*
*of*
MASTER OF TECHNOLOGY
in
ELECTRICAL ENGINEERING
(With Specialization in Power Apparatus and Electric Drives)

By
## NAGARJUN BOMMINENI

DEPARTMENT OF ELECTRICAL ENGINEERING
INDIAN INSTITUTE OF TECHNOLOGY ROORKEE
ROORKEE - 247 667 (INDIA)
JUNE, 2007

I.D. No.-M.T. ~~~~~~~~~~~~~~~~~~~~~~~~

$379/2007-12/YP-SGC$

# CANDIDATE'S DECLARATION

I hereby declare that the work that is being presented in this dissertation report entitled **"PERFORMANCE INVESTIGATIONS ON DSP BASED PERMANENT MAGNET SYNCHRONOUS MOTOR DRIVE"** submitted in partial fulfillment of the requirements for the award of the degree of **Master Of Technology** with specialization in **Power Apparatus and Electric Drives,** to the **Department Of Electrical Engineering, Indian Institute Of Technology, Roorkee,** is an authentic record of my own work carried out, under the guidance of Sri. Y. P. Singh, Asst. Professor, Department of Electrical Engineering and Dr. S. Ghatak Choudhuri, Lecturer, Department of Electrical Engineering.

The matter embodied in this dissertation report has not been submitted by me for the Award of any other degree or diploma.

Date: 22-06-2007

Place: Roorkee

(NAGARJUN BOMMINENI)

This is to certify that the above statement made by the candidate is correct to the best of my knowledge.

(Sri.Y.P.SINGH)

Asst. Professor,

Department of Electrical Engineering,

Indian Institute of Technology,

Roorkee-247667,

India.

(DR. S.GHATAK CHOUDHURI)

Lecturer,         22.06.2007

Department of Electrical Engineering,

Indian Institute of Technology,

Roorkee-247667,.

India.

# ACKNOWLEDGEMENT

I would like to thank Sri. Y.P.SINGH, Assistant Professor, Department of Electrical Engineering and Dr. S.GHATAK CHOUDHURI, Lecturer, Department of Electrical Engineering, I.I.T. Roorkee, who took great efforts in providing good guidance and was enthusiastic about my work.

I express my deep & sincere sense of gratitude to all the faculty members & institute staff. These acknowledgements would be incomplete without thanking my fellow M.Tech students for always encouraging each other to work hard.

Finally, I am indebted to my parents who have built my educational foundation, encouraged me throughout my studies and given me the choice and chance to pursue what I desired.

**DATE:** June-2007

**PLACE:** Roorkee

(NAGARJUN BOMMINENI)

# ABSTRACT

Adjustable speed drives are essential for energy savings in industries. The availability of modern permanent magnets (PM) with considerable energy density led to the development of dc machines with PM field excitation in 1950s. Traditionally DC motors have been used for the adjustable speed drives. Now-a-days vector controlled ac drives are replacing the dc drives because ac motors are more robust and need minimum maintenance due to absence of commutators and brushes. Among the ac motors permanent magnet synchronous motors (PMSM) are superior to squirrel cage induction motors for servo applications as it has fast response, higher torque to inertia ratio, higher power density and higher efficiency. Further, the permanent magnet ac motors do not need magnetizing current from stator side. The magnets on rotor are of high resistivity materials thus losses in the rotor are negligible.

In the PWM inverter fed PMSM control structure, the rotor position and speed are sensed. The actual rotor speed is subtracted from a reference speed and speed error is processed in speed controller to obtain a reference torque. The torque command is divided with the PMSM torque constant to obtain torque component (q-axis component) of the reference current. The field component (d-axis component) of the reference current is kept zero as the PMSM surface mounted type in which demagnetization is avoided. Using torque and field components of the reference current and rotor position angle, the park's transformation is applied to transform dq-axis references currents to abc-axis reference currents. The actual three phase stator currents are subtracted from the abc-axis references currents and the currents errors are passed through fed to sinusoidal pulse width modulated (SPWM) current controller, which provides controlled switching signals to the inverter switches. The controlled switching of the inverter feeds regulated current to the PMSM.

Mathematical models of the PMSM and vector control of the drive is developed. The models are used for associate controller designs and simulation of the drive. The PMSM speed controller is investigated with PI, Fuzzy, Hybrid and FPPI speed controllers. And the drive performance is compared with these speed controllers. The SPWM technique is implemented with I-8438 embedded controller.

Sensorless vector control of the drive is also simulated; in this control simple open loop flux estimator is used. Speed and rotor position are estimated with two voltages and current signals.

To summarize, a vector controlled PMSM drive is simulated with different speed controllers. And the performance of the drive is compared with different speed controllers (PI, Fuzzy, Hybrid and FPPI). Sensorless vector control of the drive is also simulated.

# CONTENTS

# List of Symbols

| | |
|---|---|
| $r_s$ | Stator phase winding resistance |
| $V_{as}, V_{bs}, V_{cs}$ | Three-Phase stator winding voltages of the PMSM |
| $i_{as}, i_{bs}, i_{cs}$ | Three-Phase stator winding currents |
| $L_{aas}, L_{bbs}, L_{ccs}$ | Magnitudes of self-inductances of stator phase windings |
| $L_{abs}, L_{bcs}, L_{cas}$ | Magnitude of mutual-inductances of stator phase windings |
| $\lambda_{sf}$ | D-axis magnetic flux due to rotor permanent magnet |
| $L_s$ | Stator phase winding inductance |
| $\omega$ | Synchronous speed in electrical Rad./Sec. |
| $\theta$ | Electrical angle in radians from stator reference axis |
| $P$ | No. of poles on the rotor |
| $K_t$ | Torque constant |
| $T_L$ | Load torque |
| $T_e$ | Electrical torque |
| B | Damping friction of the PMSM load |
| $J_m$ | Moment of inertia of the PMSM load |
| $\omega_m$ | Synchronous in mech. Rad./Sec. |
| $\theta_m$ | Mechanical angle in radians from stator reference axis |
| $V_{dc}$ | DC link voltage |
| $E_m$ | Peak amplitude of supply phase voltage |
| $\omega_m^*$ | Speed command |
| $T^*$ | Reference Torque |

# Introduction

## 1.1. General

Motion control with electrical drives is always a challenge for researchers and technologists. Nowadays, motion control system has become a vast area to be recognized as a distinct field. Adjustable speed drives are preferred over fixed speed motor because of several reasons, energy saving, velocity or position control and for good transient response etc. The contribution made by power electronics engineers is increasing day-by-day in the area of precise motion control technology with electrical actuators such as dc/ac servomotors.

In earlier days, one of the most suitable motors for servo applications was separately excited dc motor. The commutators and brushes in the dc motors imposed limitations on high-speed applications and required frequent maintenance. The sparking on commutator prohibited use of the dc motors in mines and other inflammable zones. Due to these drawbacks, the dc motors are being replaced by ac motors in most of the modern drives.

Successive advancements in motor design, control techniques and power electronics, has led to efficient modern drives. The main contribution to modern motor drives is implementation of digital controllers using microprocessors, Digital Signal Processors (DSPs), Field Programmable Gate Arrays (FPGAs) and Programmable Logic Controllers (PLCs) etc. along with high frequency switching devices like Bipolar Junction Transistors (BJTs), Insulated-gate bipolar transistors (IGBTs) and Metal Oxide Semiconductor Field Effect Transistors (MOSFETs) etc. Modern day servo drive motors include cage induction motor, trapezoidal input current permanent magnet motor, sinusoidal input current permanent magnet motor and switched reluctance motor.

The availability of modern permanent magnets (PM) with considerable energy density led to the development of dc machines with PM field excitation in 1950s. Introduction of PM to replace electromagnets, which have windings and require an external electric energy source, resulted in compact dc machines. The synchronous machine, with its conventional field excitation in the rotor, is replaced by the PM excitation; the slip rings and the brush assembly are dispensed with. The armature of the dc machine need not be

on the rotor if the mechanical commutator is replaced by its electronic version. Therefore, the armature of the machine can be on the stator, enabling better cooling and allowing higher voltages to be achieved: significant clearance space is available for insulation in the stator. The excitation field that used to be on the stator is transferred to the rotor with the PM poles. These machines are nothing but 'an inside out dc machines' with the field and armature interchanged from the stator to rotor and rotor to stator, respectively.

In the ac drives either an ac motor or a switched reluctance motor is used. The switched reluctance motor produces large torque ripples; hence, for getting smooth torque and speed characteristics either an induction motor or a permanent magnet motor is preferred. Fig.1.1 shows the classification of electric motors.
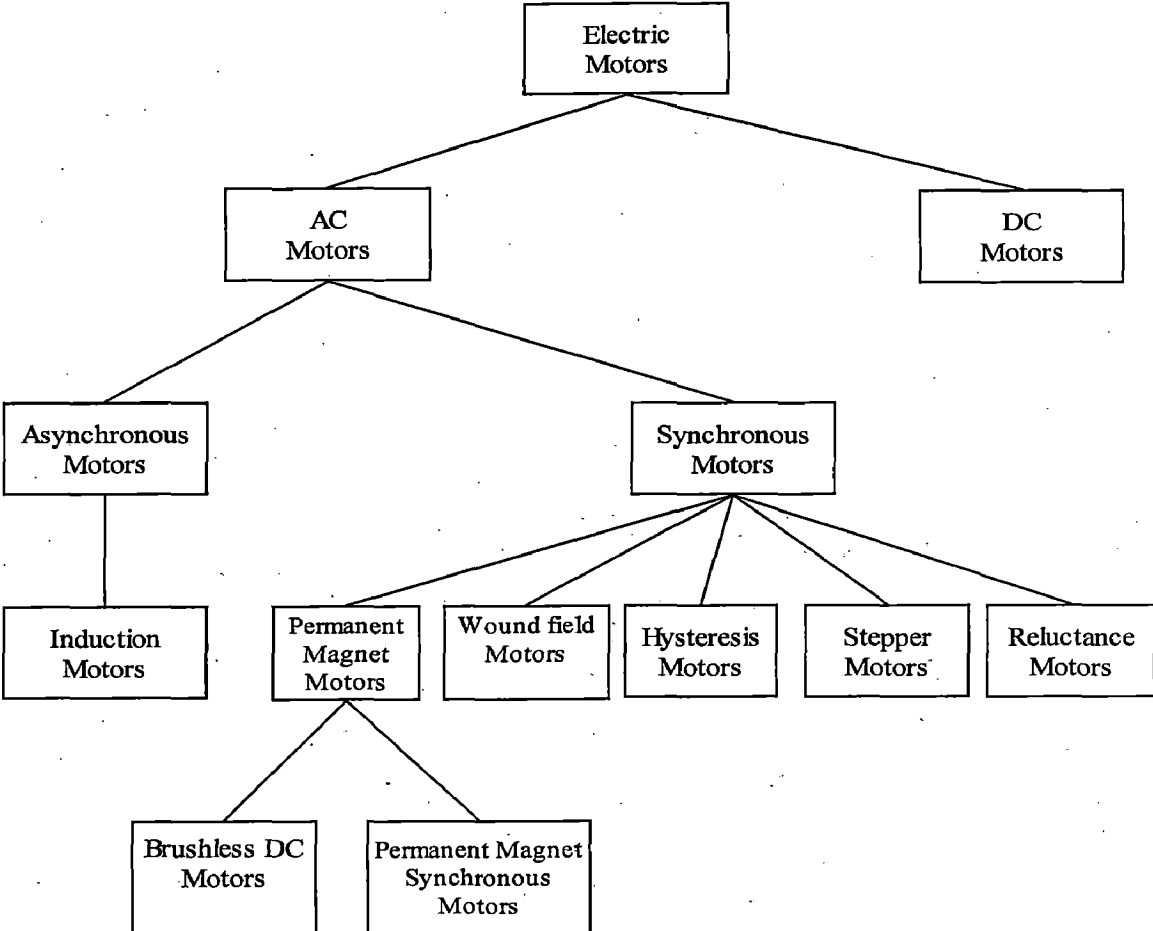


Fig.1.1 Classification of electric motors

## 1.2.Advantages of Permanent Magnet (PM) Motors :

For the same power rating, the permanent magnet motor possesses some distinct advantages over the squirrel-cage induction motor.

The rare earth and neodymium boron Permanent Magnet (PM) have lower inertia when compared with induction motors because of the absence of a rotor cage, these results in faster response for a given electric torque. In other words, the torque to inertia ratio of these PM machines is higher [11].

The PM motors have higher efficiency than induction motors [2]. This is primarily due to negligible rotor losses in permanent magnet machines; the rotor losses in the IM, however, can be considerable, depending on the operating slip. This discussion is applicable to constant flux operation.

The Induction motors need a source for excitation. The PM motors already have the excitation in the form of the rotor magnet.

For the same output capacity Induction motors have lower efficiency and require larger rated rectifiers and inverters due to excitation when compared to permanent magnet motors.

The PM motor is smaller in size than an induction motor of the same capacity. Hence, it is advantageous to use PM motors, especially where space is a serious limitation. In addition, the permanent magnet motor has less weight [5]. In other words, the power density of permanent magnet motors is higher.

The rotor losses in a PM motor are negligible when compared with induction motor rotor losses. A problem that has been encountered in the machine tools industry is the transferal of these rotor losses in the form of heat to the machine tools and work pieces, thus affecting the machining operation. This problem is avoided in permanent magnet machines.

## 1.3. Types of permanent magnet motors:

Permanent Magnet motors (PM) can be classified into two types

1. Permanent Magnet Brushless DC Motors (PMBLDCM)
2. Permanent Magnet Synchronous Motors (PMSM)

**1.3.1. PMBLDCM:** - The characteristic features of the brushless D.C. motors are

    (1) rectangular distribution of flux in the air gap

    (2) rectangular current waveforms

    (3) Concentrated stator windings.

**1.3.2. PMSM:** - The characteristic features of the permanent magnet synchronous motors are

    (1) Sinusoidal distribution of magnetic flux in the air gap

    (2) Sinusoidal current waveforms

    (3) Short-pitched and distributed or concentric stator windings.
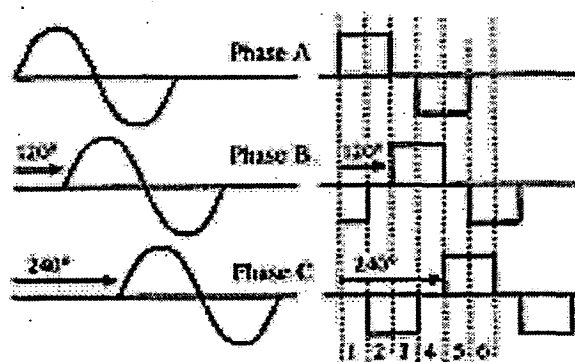


Fig.1.2 Basic excitation waveforms for (a) sinusoidal and (b) trapezoidal PMAC motors.

Fig. 1.2 provides a direct comparison of idealized current excitation waveforms for typical three-phase sinusoidal and trapezoidal PMAC motors. Despite their obvious differences in wave shape some important similarities also apparent. For example, this excitation waveforms form balanced three-phase sets for both PMAC classes, with 120 electrical degree separations between successive phases [3].

**1.4 Differences between the PMSM and PMBLDCM :**

The PMSM has a sinusoidal back emf, whereas the PMBLDCM has a trapezoidal back emf. Both have a permanent magnet rotor, but the difference is in the winding arrangement of the stator and shaping of the magnets. Sinusoidal stator currents are needed to produce a steady torque in the PMSM, whereas rectangular-shaped currents are needed to produce a steady torque in the PMBLDCM. It is this difference that has

4

numerous ramifications both in the behavior of the motor drive and in the structure of the control algorithms and circuitry [2].

The PMSM provides less torque ripples, higher speed range, more accurate speed and position control because of continuous rotor position feedback. On the other hand, the PMBLDCM has higher torque per unit current if both are operating on constant operation mode. The PMSM drives are proving more suitable for high performance adjustable speed ac drives applications. In the machine tool industry the transfer of heat due to rotor losses to the machine tools and work pieces, affects the machining operation.

Due to negligible rotor losses compared to other servo drives like; dc motor and induction motor drives, there is wide scope of the PMSM in machining applications.

### 1.5 Operation of PMSM :

The PMSM replaces field coil, dc power supply and slip rings of synchronous machine with a permanent magnet. The PMSM requires sinusoidal current to produce constant torque like a synchronous motor.
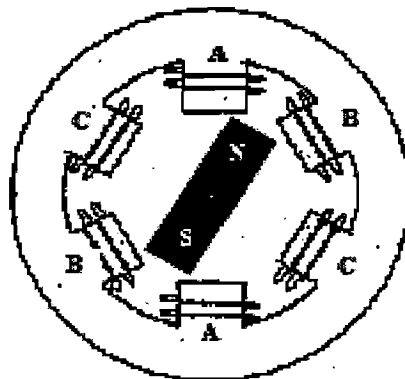


Fig1.3 Three-Phase Synchronous Motor with One Permanent Magnet Pair Pole Rotor

The interaction between the rotating stator flux and the rotor flux produces a torque which will cause the motor to rotate [5]. The rotation of the rotor in this case will be at the same exact frequency as the applied excitation to the rotor.

## 1.6. Classification of PMSM :

The PMSM is classified based on its rotor design in two categories.

(1) an exterior permanent magnet type (EPM) PMSM

(2) an interior permanent magnet type (IPM) PMSM

In EPM type of PMSM the permanent magnets are fitted on the surface of rotor periphery of the motor. This construction of PMSM is also known as Surface PMSM.

In IPM type of PMSM the permanent magnets are embedded inside the rotor.
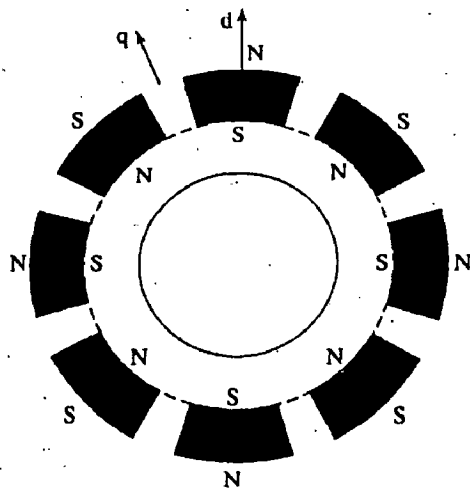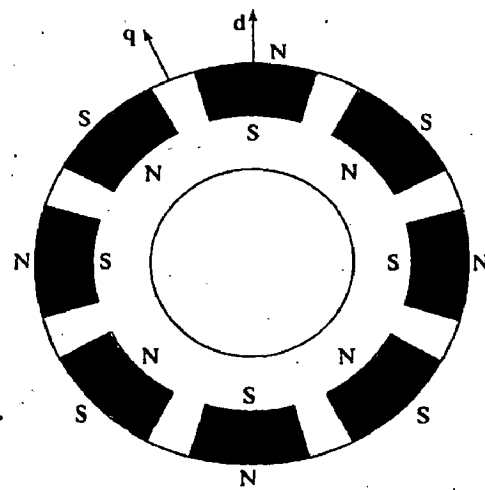


Fig.1.4 Surface PMSM      Fig.1.5 Surface inset PMSM

Fig.1.4 shows the magnets mounted on the surface of the outer periphery of rotor laminations. This arrangement provides the highest air gap flux density, but it has the drawback of lower structural integrity and mechanical robustness. Machines with this arrangement of magnets are known as surface mount PMSM s or EPM s. they are not preferred for high-speed applications, generally greater than 3,000 rpm. There is very little (less than 10%) variation between the quadrature- and direct-axis inductances in this machine. The particular fact has consequences for the control, operation and characteristics of the surface-mount PMSM drives [24].

Fig.1.5 shows the magnets placed in the grooves of the outer periphery of the rotor laminations, providing a uniform cylindrical surface of the rotor. In the addition, this arrangement is much more robust mechanically as compared to surface-mount machines.

The ration between the quadrature- and direct- axis inductances can be high as 2 to 2.5 in this machine. This construction is known as inset PM synchronous machine [5].
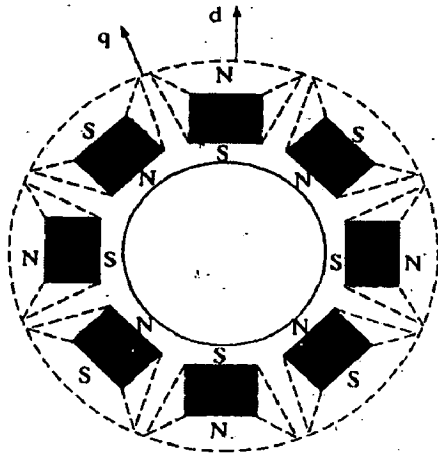


Fig.1.6 Interior PMSM
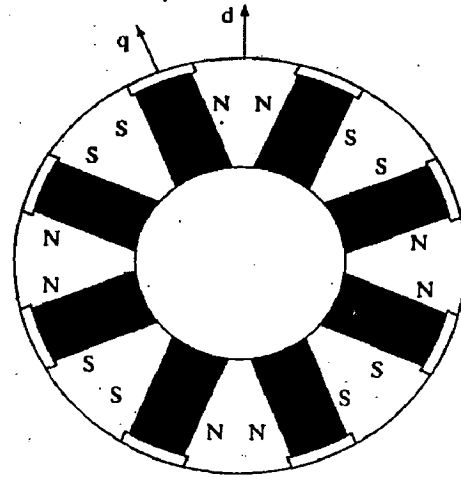
Fig.1.7 Interior PMSM with circumferential Orientation

Fig.1.6, 1.7 shows the placement of magnets in the middle of the rotor laminations in radial and circumferential orientations, respectively. This construction is mechanically robust and therefore suited for high-speed applications. The manufacturing of this arrangement is more complex than for the surface mount or inset-magnet rotors. Note that the ratio between the quadrature- and direct-axis inductances can be higher than that of the inset-magnet rotor but generally does not exceed three in value. This type of machine construction is generally referred to as interior PMSM.

## 1.7 Literature review:

In reference [2], the very basic fundamentals of the PMSM are described. The author has given the idea of construction of PMSM, the various magnetic materials used for permanent magnet rotor, types of permanent magnet motors and the characteristics of the permanent magnet synchronous motor with the help of vector diagram. In reference [24] the author has given the clear picture of applications, advantage and limitations of different configurations of PM Brushless machines.

There are two types of permanent magnet motors, PMSM and BDCM. The PMSM and BDCM have many similarities; they both have permanent magnets on the rotor and

require alternating stator currents to produce constant torque. The difference between two machines is that the PMSM and BDCM have sinusoidal and trapezoidal back emf's. Reference [11] describes the application characteristics of PMSM and BDCM; it also describes how permanent magnet motors are better than induction motors.

Reference [12] gives detailed representation of buried permanent magnet synchronous motors at steady state is presented. An equivalent circuit is proposed that accounts for saliency of the machine and for the particular influence of iron core losses on the machine operations. No-load as well as loaded conditions are analyzed and experimentally tested in order to describe the influence of the armature current on the rotor flux distribution.

The application of vector control of PMSM and complete modeling, simulation and analysis of the drive system are described in [7]. State space models of the motor and speed-controller and real-time models of the inverter switches are described.

The basic concept of vector control and application of this control to the PMSM is thoroughly explained in references [1, 3, 4] and [5].

Motion control techniques have been developed to exploit the high efficiency and extremely fast dynamic response capabilities of PMAC machines. Control techniques are reviewed separately for the two major classes of PMAC machines referred in [14]. Trapezoidal PMAC machine drives are distinguished by their controls simplicity and minimal sensor requirements, sinusoidal PMAC machine drives offers opportunities for extremely smooth torque production and extended high-speed operating ranges. Advanced PMAC machine control topics are described.

N. Senthil kumar and K. Saravanan [23], presented speed control of PMSM drive using VSI. Vector control has been used for high servo applications and this paper describes the complete scheme of PMSM drive.

F.M. Abdul–kader and S.M. Osheba [8] analyses the dynamic performance of PMSM using damping and synchronizing torques. The results illustrates the significant improvement in transient performance can be achieved, over a wide range of voltages and frequencies, when some parameters are properly chosen.

Rashid [6] explained the basic concepts of SPWM and the advantages of this technique. The analysis of PMSM shows that the increase of electromagnetic torque is

proportional to the increase of the angle between the stator and rotor angle flux linkages and there fore fast torque response can be obtained by increasing the rotating speed of the stator flux linkages as fast as possible.

In references [9, 10] the author explained the basic fundamentals of fuzzy logic, he also explained different dufuzzifications methods. In references [15] the authors explained how fuzzy logic can be implemented in speed controller and in the references [18, 21] the authors explained various speed control techniques like Hybrid controller and FPPI controller.

Vas Peter [1] explained the basic concepts and operation of the PMSM and he also discussed about the vector control and various methods of speed and rotor angle estimation techniques. In reference [17], Tomonobu Senjyu explained the open loop position and speed estimation technique. In reference [20] the authors explained the elimination of drift in the estimated flux.

In the references [19, 13] the authors had given the idea about estimation of speed and rotor position over a wide range of speed.

# Mathematical modeling of PMSM

## 2.1 Assumptions :

The assumptions made for modeling of the PMSM are as follows:

1. The three phase stator windings of the PMSM are balanced and produce sinusoidally distributed Magneto Motive Force (MMF) in the space.

2. The permanent magnets on the rotor produce sinusoidally distributed magnetic flux in the air-gap space.

3. The magnetic material is highly resistive hence; current dynamics in the rotor are neglected.

4. Saturation and iron losses in the machine are neglected.

5. The three-phase sinusoidal currents flowing into the motor are also assumed ripple free (fundamental currents are assumed to simplify the motor model).

## 2.2 PMSM model :

The stator of the PMSM is same as the stator of a synchronous motor and its rotor consists of multi-pole permanent magnets on its surface. The PMSM rotors are interior permanent magnet (IPM) type and projection permanent magnet (PPM) type. The IPM rotor possesses saliency and it provides sufficient demagnetization range as to allow operation of the motor in field weakening region also. In contrary, the projection type PM motor is not able to operate in field-weakening range because its demagnetization capability is very small. In the present model of the PMSM, projection type permanent magnet rotor is considered. The relative permeability of the permanent magnet is approximately equal to that of air. Insetting a permanent magnet on the rotor is same as introducing an air-gap equivalent to the width of the magnet. The permanent magnet on the rotor is shaped such that its flux in the air gap is almost sinusoidal. Hence, for the PPM type motor the air gap is assumed uniform throughout the rotor periphery.

## 2.2.1 Stator Reference Model of the PMSM (in M.K.S. Units) :
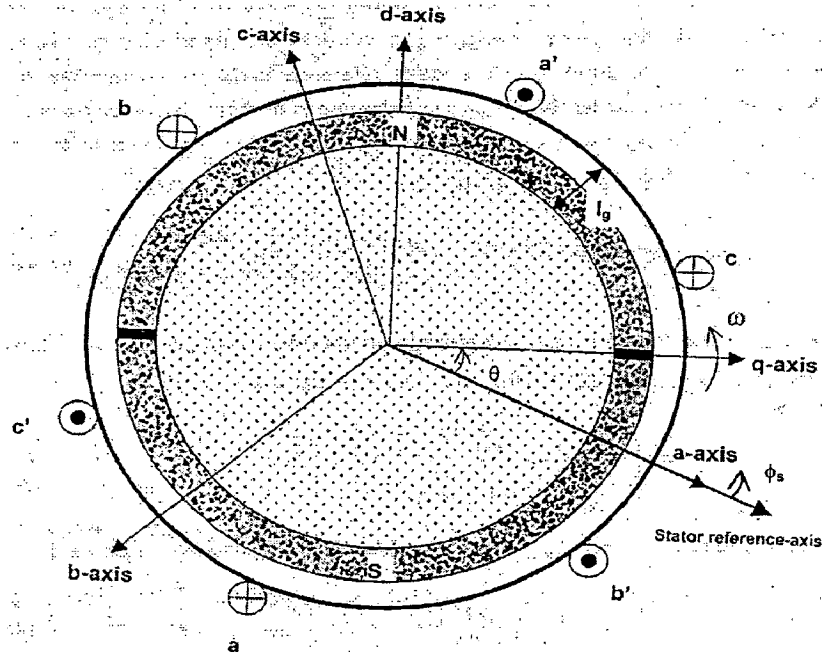


Fig.2.1 Schematic of two pole PMSM

Figure 2.1 shows a schematic diagram of the projection type PMSM. The stator phase windings are sinusoidally distributed and suitably fractional-pitched as to obtain sinusoidal air-gap flux. Small circles on the stator periphery show the stator winding conductors. To simplify the drive model, the stationary frame reference-axis and phase-'a' axis are chosen as coinciding to each other [7].

Three-phase stator reference frame voltage equations of the PMSM are written as [22]

$$\left[ \vec{V}_{abc} \right] = \left[ r_s \right] + \left[ \vec{\lambda}_{abcs} \right] \tag{2.1}$$

Where $\left[ \vec{V}_{abcs} \right] = \left[ V_{as} \quad V_{bs} \quad V_{cs} \right]^T$ ; $\left[ i_{abcs} \right] = \left[ i_{as} \quad i_{bs} \quad i_{cs} \right]^T$ ;

Rate of change of flux linkages to stator windings $\vec{\lambda}_{abcs}$ is the static as well as dynamic induced EMFs in the windings. The dot over the vector denotes its first order differentiation. The flux linkages in stator phase windings are given as

$$\left[\dot{\vec{\lambda}}_{abcs}\right]=\left[L_{abcs}\right]\left[\vec{i}_{abcs}\right]+\left[\vec{\lambda}_{abcsf}\right] \tag{2.2}$$

Where, $\vec{\lambda}_{abcsf}$ is the magnetic flux linkage vector to stator windings due to permanent magnets on the rotor, as seen from stationary reference axis. Differentiating equation (2.2) and substituting into equation (2.1), the voltage equation is written as,

$$\left[\vec{V}_{abcs}\right]=\left[r_s\right]\left[\vec{i}_{abcs}\right]+\left[L_{abcs}\right]\left[\dot{\vec{i}}_{abcs}\right]+\left[\dot{\vec{\lambda}}_{abcsf}\right] \tag{2.3}$$

Where, $\left[\vec{i}_{abcs}\right]=\begin{bmatrix} i_{as} & i_{bs} & i_{cs} \end{bmatrix}$; $\left[\vec{\lambda}_{abcsf}\right]=\lambda_{sf}\begin{bmatrix} \sin\theta \\ \sin\left(\theta-2\pi/3\right) \\ \sin\left(\theta+2\pi/3\right) \end{bmatrix}$

$$\left[r_s\right]=\begin{bmatrix} r_s & 0 & 0 \\ 0 & r_s & 0 \\ 0 & 0 & r_s \end{bmatrix}; \quad \text{and} \quad \left[L_{abcs}\right]=\begin{bmatrix} L_{aas} & L_{abs} & L_{acs} \\ L_{bas} & L_{bbs} & L_{bcs} \\ L_{cas} & L_{cbs} & L_{ccs} \end{bmatrix}$$

Since, the three phase windings are balanced, the mutual inductances of the phase windings are equal. The magnitudes of the mutual inductances are equal to half the magnitudes of self-inductances with differential flux linkage. Hence,

$$L_{abs}=L_{bas}=L_{acs}=L_{cas}=L_{cbs}=L_{bcs}=-L_s/2;$$

Substituting above values of inductances in the inductance matrix $L_{abcs}$ the new inductance matrix is,

$$\left[L_{abcs}\right]=\begin{bmatrix} L_s & -L_s/2 & -L_s/2 \\ -L_s/2 & L_s & -L_s/2 \\ -L_s/2 & -L_s/2 & L_s \end{bmatrix}$$

The dynamically induced voltages in the phase windings i.e., $\vec{\lambda}_{abcsf}$ is obtained by differentiating $\vec{\lambda}_{abcsf}$ as

$$\left[\vec{\lambda}_{abcsf}\right] = \omega\lambda_{sf}\begin{bmatrix} \cos\theta \\ \cos(\theta - 2\pi/3) \\ \cos(\theta + 2\pi/3) \end{bmatrix}$$

Where, $\lambda_{sf}$ is the flux linkage produced by the permanent magnet of the rotor as viewed from the stator windings and $\omega$ is speed of the rotor flux.

### 2.2.2 Rotor Reference Model of the PMSM (in M.K.S. Units) :

Using the *Park's* transformation, three-phase voltages and currents of the stator windings of the motor are transformed to the rotor reference frame as [22]

$$\left[\vec{V}_{qd0}\right] = K_s\left[\vec{V}_{abcs}\right] \qquad (2.4.1)$$

$$\left[\vec{i}_{qd0}\right] = K_s\left[\vec{i}_{abcs}\right] \qquad (2.4.2)$$

The voltages and currents of the rotor reference frame are transformed to the stator reference frame using the inverse Park's transformation as

$$\left[\vec{V}_{abcs}\right] = K_s^{-1}\left[\vec{V}_{qd0}\right] \qquad (2.5.1)$$

$$\left[\vec{i}_{abcs}\right] = K_s^{-1}\left[\vec{i}_{qd0}\right] \qquad (2.5.2)$$

Where, $K_s = \dfrac{2}{3}\begin{bmatrix} \cos\theta & \cos(\theta - 2\pi/3) & \cos(\theta + 2\pi/3) \\ \sin\theta & \sin(\theta - 2\pi/3) & \sin(\theta + 2\pi/3) \\ 1/2 & 1/2 & 1/2 \end{bmatrix}$

And $K_s^{-1} = \begin{bmatrix} \cos\theta & \sin\theta & 1 \\ \cos(\theta - 2\pi/3) & \sin(\theta - 2\pi/3) & 1 \\ \cos(\theta + 2\pi/3) & \sin(\theta + 2\pi/3) & 1 \end{bmatrix}$

The waveforms of the voltages, currents and flux linkages depend on the reference frame chosen, but the waveform of power is always the same for any reference frame. The transformation from one reference frame to other is always power invariant. Equating

instantaneous power in the stator reference frame to instantaneous power in the rotor reference frame, using equations (2.4.1 & 2.4.2) we obtain,

$$V_{as}i_{as} + V_{bs}i_{bs} + V_{cs}i_{cs} = \frac{3}{2}\left(V_{qs}i_{qs} + V_{ds}i_{ds}\right) \tag{2.6}$$

The constant factor 3/2 yields from the Park's transformation chosen. Using the Park's transformation, the three-phase voltages and currents are transferred to the rotor reference frame i.e., to d-q-0 axis. The stator reference frame parameters like stator resistances and stator inductances are also transformed to the rotor reference frame. The transformation of voltage equation (2.1) from the stator reference frame to the rotor reference frame is given as

$$\left[\vec{V}_{qd0}\right] = K_s\left[r_s\right]K_s^{-1}\left[\vec{i}_{qd0}\right] + K_s\frac{d}{dt}\left\{K_s^{-1}\left[\vec{\lambda}_{qd0}\right]\right\} \tag{2.7}$$

Where, $\vec{\lambda}_{qd0}$ is the rotor magnetic flux referred on the rotor reference-axis. Transferring the parameters of equation (2.2) to the rotor reference frame it is written as

$$\left[\vec{\lambda}_{qd0}\right] = K_s\left[L_{abcs}\right]K_s^{-1}\left[\vec{i}_{qd0}\right] + \left[\vec{\lambda}_{abcsf}\right] \tag{2.8}$$

Substituting the values of $K_s, K_s^{-1}, L_{abcs}$ and $\left[\vec{\lambda}_{abcsf}\right]$ and simplifying equation (2.8), we get

$$\left[\vec{\lambda}_{qd0s}\right] = \left[L_{qd0}\right]\left[\vec{i}_{qd0}\right] + \left[\vec{\lambda}_f\right] \tag{2.9}$$

Where, $\left[\vec{\lambda}_f\right] = \begin{bmatrix} 0 \\ \lambda_{sf} \\ 0 \end{bmatrix}; \left[L_{dq0}\right] = \begin{bmatrix} L_q & 0 & 0 \\ 0 & L_d & 0 \\ 0 & 0 & 0 \end{bmatrix}$ and $L_q = L_d = L_s$ for projection permanent

magnet type rotor. Substituting equation (2.9) into equation (2.7), we obtain,

$$\left[\vec{V}_{qd0}\right] = \left[r_s\right]\left[\vec{i}_{qd0}\right] + \left[L_{qd0}\right]\left[\vec{i}_{qd0}\right] + K_sK_s^{-1}\frac{d}{dt}\left\{\left[L_{qd0}\right]\left[\vec{i}_{qd0}\right] + \left[\vec{\lambda}_f\right]\right\}$$

$$+ K_s\frac{d}{dt}\left[K_s^{-1}\right]\left\{\left[L_{qd0}\right]\left[\vec{i}_{qd0}\right] + \left[\vec{\lambda}_f\right]\right\} \tag{2.10}$$

Where, $\frac{d}{dt}\left[K_s^{-1}\right] = \omega\begin{bmatrix} -\sin\theta & \cos\theta & 0 \\ -\sin(\theta - 2\pi/3) & \cos(\theta - 2\pi/3) & 0 \\ -\sin(\theta + 2\pi/3) & \cos(\theta + 2\pi/3) & 0 \end{bmatrix}$

14

Simplifying equation (2.10), we get

$$
\begin{bmatrix} V_q \\ V_d \\ V_0 \end{bmatrix} = \begin{bmatrix} r_s & 0 & 0 \\ 0 & r_s & 0 \\ 0 & 0 & r_s \end{bmatrix} \begin{bmatrix} i_q \\ i_d \\ i_o \end{bmatrix} + \begin{bmatrix} L_q & 0 & 0 \\ 0 & L_d & 0 \\ 0 & 0 & 0 \end{bmatrix} \begin{bmatrix} \dot{i}_q \\ \dot{i}_d \\ \dot{i}_o \end{bmatrix} + \omega \begin{bmatrix} 0 & L_d & 0 \\ -L_q & 0 & 0 \\ 0 & 0 & 0 \end{bmatrix} \begin{bmatrix} i_q \\ i_d \\ i_o \end{bmatrix} + \omega \begin{bmatrix} \lambda_{sf} \\ 0 \\ 0 \end{bmatrix} \quad (2.11)
$$

Since, the motor operates with a three-phase balanced power supply hence, no neutral current flows i.e. $i_0 = 0$ and $V_0 = 0$ gives the q and d-axis voltages as

$$ V_q = r_s i_q + L_q \dot{i}_q + \omega L_d i_d + \omega \lambda_{sf} \tag{2.12} $$

$$ V_d = r_s i_d + L_d \dot{i}_d - \omega L_q i_q \tag{2.13} $$

Where, q-axis flux linkage is $\left( L_q i_q \right)$ and d-axis flux linkage is $\left( L_d i_d + \lambda_{sf} \right)$. Hence, electromagnetic of the motor is given as

$$ T_e = \frac{ElectricPowerOutput}{MechanicalSpeed} = \frac{(3/2) \left[ \left( \omega L_d i_d + \omega \lambda_{sf} \right) i_q - \omega L_q i_q i_d \right]}{\omega (2/P)} \tag{2.14} $$

Where, P is the no. of poles. To avoid demagnetization of permanent magnet of the rotor, the d-axis current component is kept zero by the vector control action of the drive. Hence, keeping $i_d = 0$ in the equations (2.12), (2.13) and (2.14), these are written as

$$ V_q = r_s i_q + L_q \dot{i}_q + \omega \lambda_{sf} \tag{2.15} $$

$$ V_d = -\omega L_q i_q \tag{2.16} $$

$$ T_e = \left( \frac{3P}{4} \lambda_{sf} \right) i_q = K_t i_q \tag{2.17} $$

Where, $K_t$ is the torque constant of the PMSM.

The motor load torque dynamic equation is written as,

$$ T_e = T_L + B\omega_m + J_m \frac{d\omega_m}{dt} \tag{2.18} $$

Where, $T_e, \omega_m, J_m$ and B are load torque, mechanical speed of the rotor, moment of inertia and damping friction respectively.

15

# Vector Control of PMSM

## 3.1 General structure of drive system:

The general structure of a 'motion control system' or 'drive' is shown in below fig.3.1
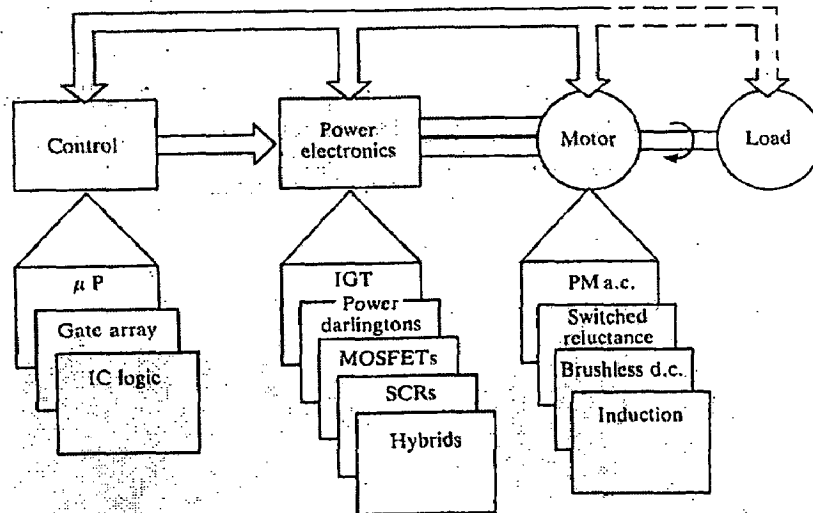


Fig.3.1 Structure of an adjustable speed drive system

The system is integrated from four distinct elements:

1. The load;

2. The motor;

3. The power electronic converter/inverter; and

4. The control.

## 3.2 VECTOR CONTROL OF PMSM:

### 3.2.1 Introduction:

Separately-excited dc drives are simpler in control because they independently control flux, which, when maintained constant, contributes to an independent control of torque. This is made possible with separate control of field and armature currents which, in turn, control the field flux and torque independently. Moreover, the dc motor control requires

only the control of the field or armature current magnitudes, providing a simplicity which is not possible with ac machine control. In ac machines because of the stator current magnitudes, frequencies and phases the control is very complex. As with the dc drives, independent control of the flux and torque is possible in ac drives. The stator current phasor can be resolved, say, along the rotor flux linkages, and the component along the rotor flux linkages is the field-producing current, but this requires the position of the rotor flux linkages at every instant; this is dynamic unlike. If this is available, then the control of the ac machine is very similar to that of separately-excited dc machines.

The requirement of phase, frequency and magnitude control of the currents and hence of the flux phasor is made possible by inverter control. The control is achieved in field coordinates (hence the name of the control strategy, *field oriented control*); sometimes it is known as *vector control,* because it relates to the phasor control of the rotor flux linkages [5].

Vector control method has the following advantages:

1. Vector control made the ac drives equivalent to dc drives in the independent control of flux and torque.

2. With this control we can obtain good dynamic performance.

### 3.2.2 Vector control:

The stator equations of the induction machine in the rotor reference frames using flux linkages are taken to derive the model of the PMSM. The rotor frame of reference is chosen because the position of the rotor magnets determines, independently of the stator voltages and currents, the instantaneous induced emfs and subsequently the stator currents and torque of the machine.

The electromagnetic torque (eqn. 2.14) of the machine is given by

$$T_e = \frac{3}{2}\frac{P}{2}\left\{\lambda_{ds}^r i_{qs}^r - \lambda_{qs}^r i_{ds}^r\right\} \tag{3.1}$$

Superscript 'r' represents the rotor reference model.

The permanent magnet-excitation is modeled as a constant current source $i_{fr}$. The rotor flux is along the d-axis, so the d-axis rotor current $i_{fr}$. The q-axis current in the rotor is zero, because there is no flux along this axis in the rotor, by assumption.

Then the flux linkages are written as

$$\lambda_{qs}^r = L_q i_{qs}^r \tag{3.2}$$

$$\lambda_{ds}^r = L_d i_{ds}^r + L_m i_{fr} \tag{3.3}$$

Where, $L_m$ is the mutual inductance between the stator winding and the permanent magnet.

Substituting equations 3.2, 3.3 in 3.1, we get the following equation

$$T_e = \frac{3}{2}\frac{P}{2}\left\{\lambda_{af} i_{qs}^r + \left(L_d - L_q\right) i_{qs}^r i_{ds}^r\right\} \tag{3.4}$$

Where the rotor flux linkages that link the stator are

$$\lambda_{af} = L_m i_{fr} \tag{3.5}$$

Considering the currents as inputs, the three phase currents are

$$i_{as} = i_s \sin\left(\omega_r t + \delta\right) \tag{3.6}$$

$$i_{bs} = i_s \sin\left(\omega_r t + \delta - 2\pi/3\right) \tag{3.7}$$

$$i_{cs} = i_s \sin\left(\omega_r t + \delta + 2\pi/3\right) \tag{3.8}$$

Where,

$\omega_r$ is the electrical rotor speed ,

$\delta$ is the angle between the rotor field and stator current phasor (torque angle).

The rotor field is traveling at a speed of $\omega_r$ rad./sec. hence; the q- and d- axis stator currents in the rotor reference frame for a balanced three phase operation are given by,

$$\begin{bmatrix} i_{qs}^r \\ i_{ds}^r \end{bmatrix} = \frac{2}{3}\begin{bmatrix} \cos\omega_r t & \cos\left(\omega_r t - 2\pi/3\right) & \cos\left(\omega_r t + 2\pi/3\right) \\ \sin\omega_r t & \sin\left(\omega_r t - 2\pi/3\right) & \sin\left(\omega_r t + 2\pi/3\right) \end{bmatrix}\begin{bmatrix} i_{as} \\ i_{bs} \\ i_{cs} \end{bmatrix} \tag{3.9}$$

Substituting the equations 3.6, 3.7, 3.8 in 3.9 gives the stator currents in the rotor reference frames:

18

$$\begin{bmatrix} i_{qs}^r \\ i_{ds}^r \end{bmatrix} = i_s \begin{bmatrix} \sin \delta \\ \cos \delta \end{bmatrix} \qquad\qquad (3.10)$$

The q and d axes currents are constants in rotor reference frames, since $\delta$ is a constant for a given load torque. As these are constants, they are very similar to armature and field currents in the separately-excited machine. The q axis current is distinctly equivalent to the armature current of the dc machine; the d axis current is field current, but not in it's entirely. The other part is contributed by the equivalent current source representing the permanent magnet field [4].

For $\delta = \pi / 2$

$$i_{qs}^r = i_s$$

$$i_{ds}^r = 0$$

By substituting these values in torque equation (3.4), we get

$$T_e = \frac{3}{2}\frac{P}{2}\lambda_{af} i_s = K_1 \lambda_{af} i_s \quad \text{N-m} \qquad\qquad (3.11)$$

Where $K_1 = \frac{3}{2}\frac{P}{2}$

The above equation (3.11) is similar to the torque generated in the dc motor. If the torque angle is maintained at $90^0$ and flux is kept constant, then the torque is controlled by the stator-current magnitude, giving an operation very similar to that of the armature-controlled separately-excited dc motor.

The electromagnetic torque is positive for the motoring action, if $\delta$ is positive. The rotor flux linkages $\lambda_{af}$ are positive. Then the phasor diagram for torque angle $\delta = 90^0$ is shown in below fig.3.2

$i_{qs}^r$ = Torque producing component of stator current = $i_T$

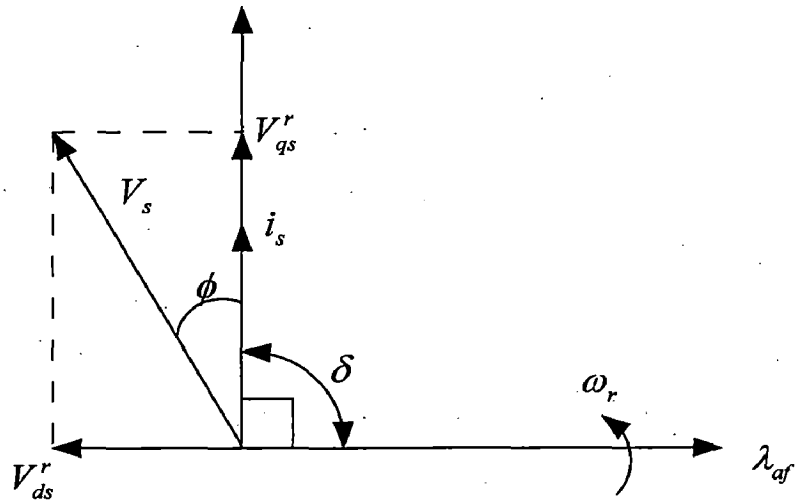$i_{ds}^r$ = Flux producing component of stator current = $i_f$

Fig 3.2 Phasor diagram of the PM synchronous machine for $\delta = 90^0$

The torque reference is a function of the speed error, and the speed controller usually of PI type. When reference torque is divided with the torque constant ($K_t$) we will get the torque component of stator current ($i_{qs}^*$) and the flux component ($i_{ds}^*$) of the stator current is always zero for PMSM Drive to avoid the demagnetization and these two components are converted in to the reference currents $i_{as}^*, i_{bs}^*$ and $i_{cs}^*$ in stationary reference frame [5]. For current control of VSI fed vector controlled PMSM, the reference currents ($i_{as}^*, i_{bs}^*$ and $i_{cs}^*$) and sensed winding currents ($i_{as}$ and $i_{bs}$) are fed into the Pulse Width Modulated (PWM) current controller. A triangular carrier wave form is generated at the required switching frequency ($f_s$). The point of intersection of the triangular carrier wave and the modulating signals acts as the point of state changeover for the PWM signals, which are fed to the driver circuit of the MOSFET of VSI feeding PMSM.

20

# Modeling and Implementation of Vector Controlled PMSM Drive in MATLAB Environment

## 4.1 Description and Modeling of vector controlled PMSM Drive:

Fig.4.1 shows the basic building block diagram of the Vector Controlled Permanent Magnet Synchronous Motor Drive (VCPMSMD). The system consists of an outer speed feedback loop and an inner current feed back loop. Two of the three phase current signals ($i_{as}$ and $i_{bs}$) along with the speed signal ($\omega_r$) are sensed and are used as feed back signals.

The speed of the motor ($\omega_r$) is compared with its reference value ($\omega_r^*$) and the error is processed in the speed controller. A limiter is kept on the output of the speed controller depending on the maximum permissible torque developed by the motor. The output of the speed controller (T) after limiting is considered as the reference torque ($T^*$).

When reference torque is divided with the torque constant ($K_t$) we will get the torque component of stator current ($i_{qs}^*$) and the flux component ($i_{ds}^*$) of the stator current is always zero for PMSM Drive to avoid the demagnetization and these two components are converted in to the reference currents $i_{as}^*, i_{bs}^*$ and $i_{cs}^*$ in stationary reference frame.

For current control of VSI fed vector controlled PMSM, the reference currents ($i_{as}^*, i_{bs}^*$ and $i_{cs}^*$) and sensed winding currents ($i_{as}$ and $i_{bs}$) are fed into the Pulse Width Modulated (PWM) current controller. A triangular carrier wave form is generated at the required switching frequency ($f_s$). The point of intersection of the triangular carrier wave and the modulating signals acts as the point of state changeover for the PWM signals, which are fed to the driver circuit of the MOSFET of VSI feeding PMSM.

Each component of the Vector controlled PMSM Drive (VCPMSMD) is modeled by a set of mathematical equations. Such set of equations when combined together represents the mathematical modeling of the complete VCPMSMD. The modeling of different components of the drive system is as follows.
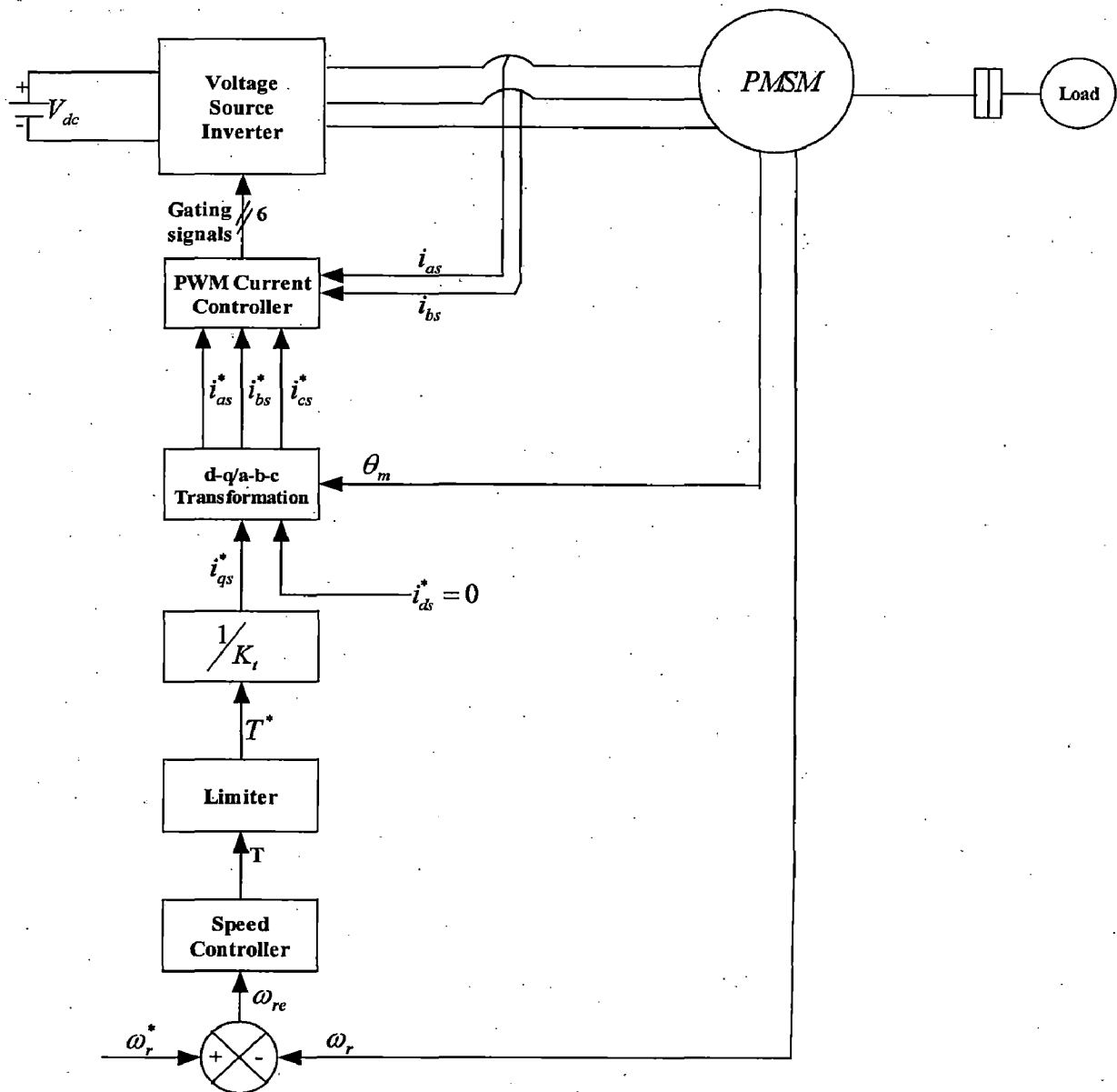
Fig 4.1 Block diagram of Vector controlled PM synchronous motor drive

### 4.1.1 Speed Controller:

The desired reference value of speed signal $\left(\omega_r^*\right)$ is compared with the feedback speed signal $\left(\omega_r\right)$ and the speed error $\left(\omega_{re}\right)$ is computed and used as an input to the speed controller, which outputs the torque value (T). The different speed controllers namely, the proportional integral (PI) speed controller, the Fuzzy Logic (FL) speed controller, the Hybrid speed controller and the Fuzzy Pre-compensated Proportional Integral (FPPI)

speed controller are used in vector controlled PMSM Drive. The output value of the torque (T) is fed to the limiter and the final reference torque $(T^*)$ is obtained from the limiter. The speed error at the $n^{th}$ instant of time is given as [21]:

$$\omega_{re(n)} = \omega^*_{r(n)} - \omega_{r(n)} \tag{4.1}$$

Where $\omega^*_{r(n)}$ : Reference speed at the $n^{th}$ instant

$\omega_{r(n)}$ : Rotor speed at the $n^{th}$ instant

$\omega_{re(n)}$ : Speed error at the $n^{th}$ instant

### 4.1.1.1 Proportional Integral (PI) speed controller:

The general block diagram of the PI speed controller shown in fig 4.2 the output of the speed controller at the $n^{th}$ instant is given as [21]:

$$T_{(n)} = T^*_{(n-1)} + K_p\{\omega_{re(n)} - \omega_{re(n-1)}\} + K_i\omega_{re(n)} \tag{4.2}$$

Where $K_p$ : Proportional gain of the PI controller

$K_i$ : Integral gain of the PI controller

The gain parameters are adjusted by observing their effects on the response on the drive.
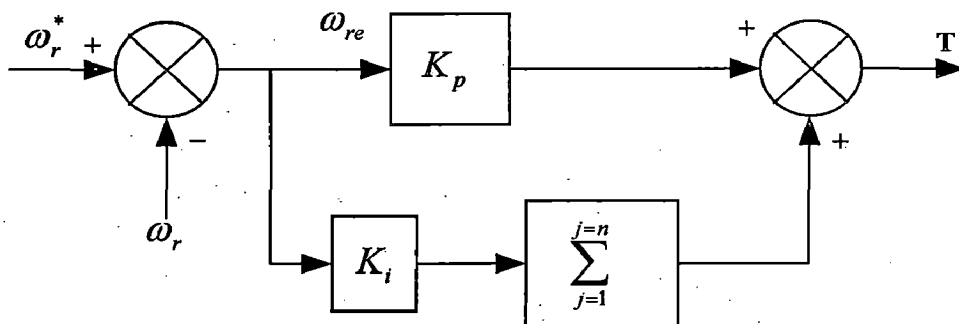


Fig.4.2 Schematic Block diagram of PI speed controller

### 4.1.1.2 Fuzzy Logic (FL) speed controller:

The internal structure of the FL speed controller is shown in Fig.4.3. It comprises of three functional blocks namely, the fuzzifier, the decision maker, and the defuzzifier. The necessary inputs are applied to these blocks [15].

The fuzzifier converts crisp data into linguistic format. The decision-maker decides in linguistic format with the help of logical linguistic rules supplied by the rule base and the relevant data supplied by the data base. The output of the decision-maker passes through

the defuzzifier wherein the linguistic format signal is converted back into the numeric form or crisp form. The decision making block uses the rules in the format of "if-then-else".

The fuzzy logic algorithm uses following steps:

1) Calculation of speed error at n[th] instant ($\omega_{re(n)}$) and change in speed error ($\Delta\omega_{re}$) as input variables.

$$\omega_{re(n)} = \omega^{*}_{r(n)} - \omega_{r(n)}$$

Change of error $\Delta\omega_{re} = \omega_{re(n)} - \omega_{re(n-1)}$

2) Appropriate scaling of the input variables $\omega_{re(n)}$ and $\Delta\omega_{re}$. The scaling is essential to bring input values into a numerical interval in which the fuzzy variables are described also known as universe of discourse.

3) The input variables are converted into labels of fuzzy sets in terms of suitable linguistic values, this is called fuzzification process. The scaled inputs are crisp values limited to the universe of discourse of input variables. The fuzzified value is a fuzzy degree of membership in the qualifying linguistic set (between 0 and 1). Triangular membership function is chosen to evaluate the degree of membership of the input crisp values.

4) In accordance with the linguistic rules, value of the output signal is determined. The required rules and data are supplied by the rule base and the data base.

5) The linguistic output data is converted back into crisp output data by application of the method of defuzzification as follows [9]:

Given a combination of two inputs, the membership of the corresponding output is taken as minimum membership value of the two respective inputs. Mathematically,

$$\alpha = \min\left[\mu(input1), \mu(input2)\right]$$

Crisp value $= \left\{\sum p(m)\alpha\right\}\Big/\sum \alpha$

Where $\mu$ refers to membership value, the output membership is stored in $\alpha$ and p(m) refers to location of peak of membership function.

6) The defuzzified (crisp) value is multiplied by a scale factor to obtain the controlled output, which is considered as the reference torque ($T^*$).
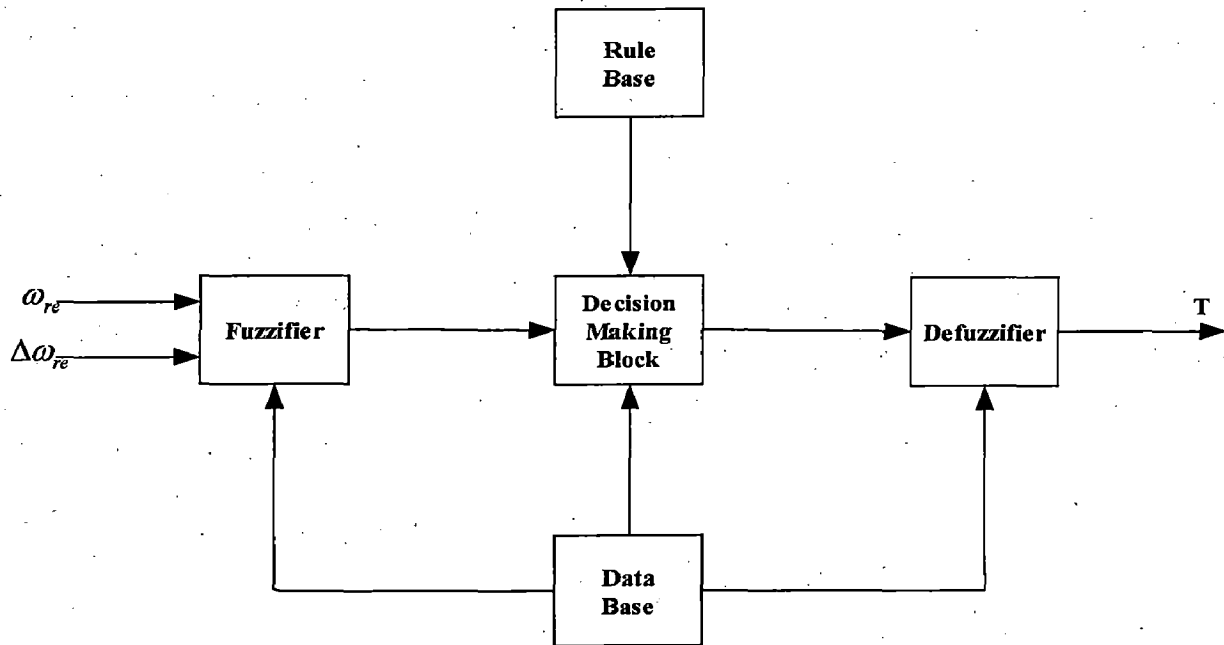


Fig.4.3 Schematic Block diagram of Fuzzy Logic (FL) speed controller

**Definition of Membership Function for Input and Output Variables:**

In the fuzzy controller of the PMSM drive, the inputs are speed error and change in speed error and thee output of the controller is the reference torque ($T^*$). The range and behavior of the input variables of the fuzzy controller are not defined. The speed error input is multiplied by a scaling factor and limited between +1 and -1. Similarly, the change is error is also multiplied by a scaling factor to limit its value between +1 and -1. The defuzzified output of the controller is within the range of +1 and -1.These input variables are denoted by E and $\Delta E$. Multiplying the defuzzified output with scale factor gives out $T^*$. Selection of suitable scale factors is important to obtain a good speed response of the PMSMD.

The membership function for input and output variables is chosen as triangular function for simplicity. The membership functions are distributed evenly in the universe of discourse. The universe of discourse for speed error input is (-1, +1), for change in speed error input is (-1, +1) and also for the output variable it is (-1, +1). Fig.4.4 shows seven terms of input and output variables by triangular shaped fuzzy membership function. The

maximum amplitude of the membership function is 1; hence, the measurements of membership range of input variables are from 0 to1 [16].
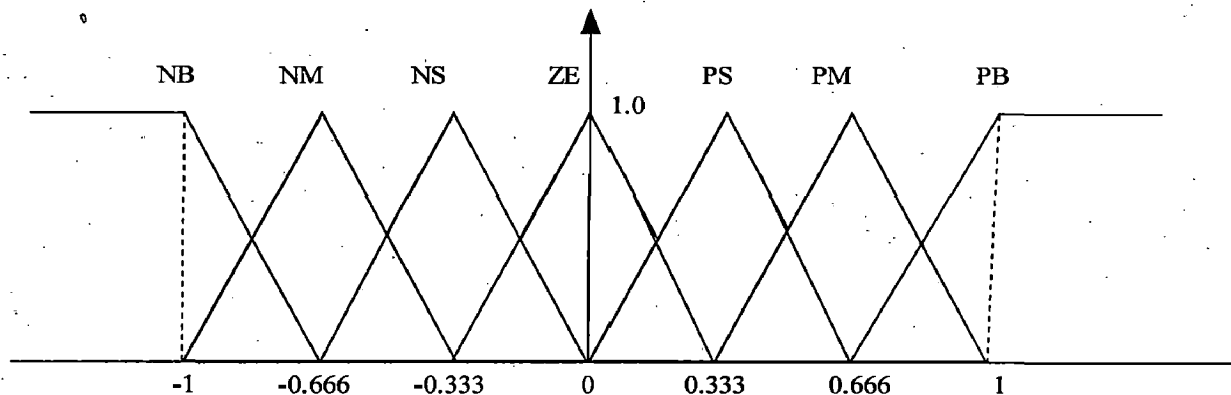


Fig 4.4 Seven term fuzzy quantization of input and output variables with triangular Shaped membership function

**Fuzzy Rule Base:**

The formation of the rule-base matrix is based on experience of human operator expert in the area of drives control. A seven-term rule base matrix is chosen from reference [16] and the formed rule base is shown in table 4.1. The order of the rule base matrix is 7X7, hence, there are forty nine rules for each combination of error (E) and change in error ($\Delta E$). The observations NB, NM, NS, ZE, PS, PM and PB are negative big, negative medium, negative small, equal to zero, positive small, positive medium and positive big respectively. All rules of the fuzzy rule base matrix can be expressed in linguistic set.

| | | E | | | | | | |
|---|---|---|---|---|---|---|---|---|
| | | NB | NM | NS | ZE | PS | PM | PB |
| $\Delta E$ | NB | NB | NB | NM | NM | NS | NS | ZE |
| | NM | NB | NB | NM | NS | NS | ZE | PS |
| | NS | NB | NB | NS | NS | ZE | PS | PM |
| | ZE | NB | NM | NS | ZE | PS | PM | PB |
| | PS | NM | NS | ZE | PS | PS | PB | PB |
| | PM | NS | ZE | PS | PS | PM | PB | PB |
| | PB | ZE | PS | PS | PM | PM | PB | PB |

Table 4.1: Fuzzy rule base matrix

**Formation of the Rule Base Matrix with Numeral Values:**

The seven level input and output variables and triangular membership function are shown in fig 4.4. The scaled inputs, speed error and change in speed error are saturated between +1 and -1 boundaries respectively. Each linguistic terms of the fuzzy rule base matrix is assigned a numerical value. Table 4.2 shows the seven level linguistic representations of the inputs and outputs, and their corresponding numerical values. The linguistic representation of the rule base is also converted into numerical values by substituting numerical values of inputs E and $\Delta E$ from table 4.2 to table 4.1; the numerical form of rule base matrix is obtained as shown in table 4.3.

| | NB | NM | NS | ZE | PS | PM | PB |
|---|---|---|---|---|---|---|---|
| **E** | -1 | -0.66 | -0.33 | 0 | 0.33 | 0.66 | 1 |
| $\Delta E$ | -1 | -0.66 | -0.33 | 0 | 0.33 | 0.66 | 1 |
| **T** | -1 | -0.66 | -0.33 | 0 | 0.33 | 0.66 | 1 |

Table 4.2: 7-term inputs and outputs of the fuzzy controller

| | | E | | | | | | |
|---|---|---|---|---|---|---|---|---|
| | | **-1** | **-0.66** | **-0.33** | **0** | **0.33** | **0.66** | **1** |
| | **-1** | -1.0 | -1.0 | -0.66 | -0.66 | -0.33 | -0.33 | 0 |
| | **-0.66** | -1.0 | -1.0 | -0.66 | -0.33 | -0.33 | 0 | 0.33 |
| $\Delta E$ | **-0.33** | -1.0 | -1.0 | -0.33 | -0.33 | 0 | 0.33 | 0.66 |
| | **0** | -1.0 | -0.66 | -0.33 | 0 | 0.33 | 0.66 | 1.0 |
| | **0.33** | -0.66 | -0.33 | 0 | 0.33 | 0.33 | 1.0 | 1.0 |
| | **0.66** | -0.33 | 0 | 0.33 | 0.33 | 0.66 | 1.0 | 1.0 |
| | **1** | 0 | 0.33 | 0.33 | 0.66 | 0.66 | 1.0 | 1.0 |

Table 4.3: The 7X7 order of fuzzy rule base matrix with numerical value

### 4.1.1.3 Hybrid speed controller:

The major disadvantage of FL control is the presence of steady state speed error on load. To eliminate this disadvantage it is necessary to combine the FL control with another suitable control technique, which is capable of removing the disadvantage existing with FL control. Therefore, a PI controller is used in combination with FL such that at the

operating point the PI controller takes over eliminating the disadvantage of FL controller. Similarly, when away from the operating point i.e. when error is high FL controller dominates and eliminates the errors due to PI controller such as occurrence of overshoots and undershoots in drives response. Such a speed controller where weighted combination of two controller outputs contributes to the net output is called hybrid speed controller. Fig.4.5 shows the block diagram of the hybrid speed controller. Fig.4.6 shows the pattern for combining the outputs of PI and FL speed controllers to realize hybrid speed controller.
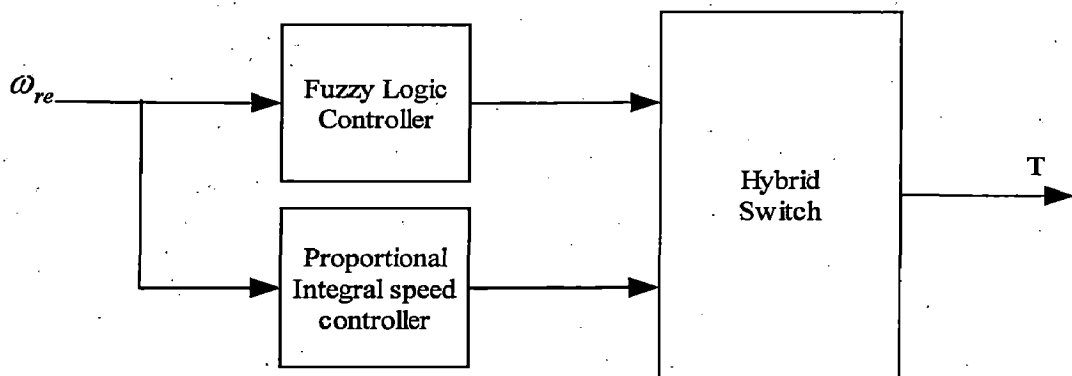


Fig.4.5. Schematic Block diagram of Hybrid Speed controller

In the p.u. speed error scale, when the error is above 1.0 pu or below -1.0 pu, the FL speed controller works. At the operating point PI speed controller is predominant [25]. For ease of mathematical calculation, four sub regions in the combination patterns of PI and FL speed controllers are defined as shown in fig.4.6.
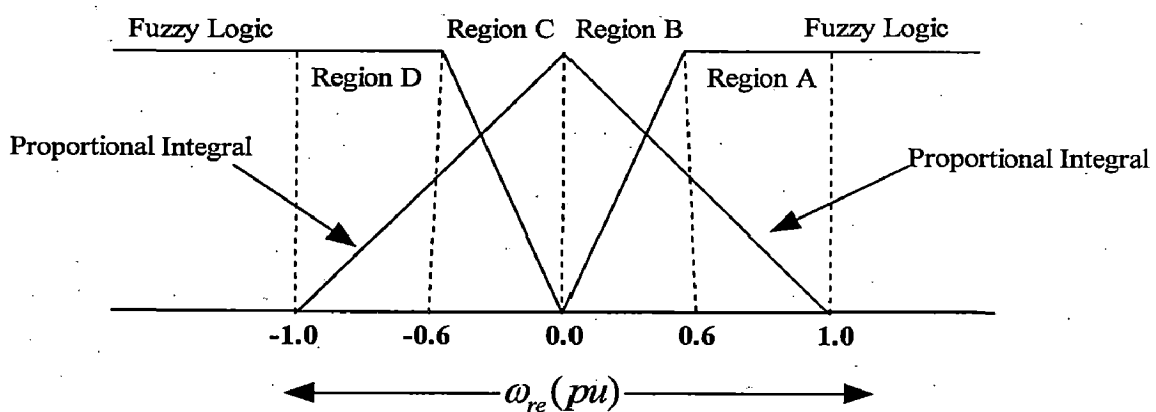


Fig.4.6 Membership function of Hybrid Fuzzy PI speed controller

Region A: Speed error between 0.666 pu and 1.0 pu

$$W_{FL} = 1.0$$

$$W_{PI} = 1 - \omega_{re(pu)}$$

Region B: Speed error between 0.0 pu and 0.666 pu

$$W_{FL} = \left(\frac{1}{0.666}\right) \omega_{re(pu)}$$

$$W_{PI} = 1 - \omega_{re(pu)}$$

Region C: Speed error between -0.666 pu and 0.0 pu

$$W_{FL} = \left(\frac{-1}{0.666}\right) \omega_{re(pu)}$$

$$W_{PI} = 1 + \omega_{re(pu)}$$

Region D: Speed error between -1.0 pu and -0.666 pu

$$W_{FL} = 1.0$$

$$W_{PI} = 1 + \omega_{re(pu)}$$

Where $W_{FL}$ refers to the weight of Fuzzy Logic speed controller

$W_{PI}$ Refers to the weight of PI speed controller

$W_{re(pu)}$ Refers to the speed error in pu scale.

The net torque output of the hybrid speed controller is expressed as [21]:

$$T_K = W_{FLK} T_{FLK}^* + W_{PIK} T_{PIK}^*$$

Where k = A, B, C, D.

When speed error greater than 1.0 pu or less than -1.0 pu

$$W_{FL} = 1.0$$

$$W_{PI} = 0.0$$

$T_{FLK}^*$ refers to the torque output of the FL speed controller (after application of speed limit) in the k$^{th}$ region of the combination pattern, $T_{PIK}^*$ refers to the torque output of the PI speed controller (after application of speed limit) in the k$^{th}$ region of the combination pattern and $T_K$ refers to the net output torque of the hybrid speed controller from the k$^{th}$ region of the combination pattern fed to the limiter.

## 4.1.1.4 Fuzzy Pre-compensated Proportional Integral (FPPI) speed controller:

PI speed controller is generally used in implementation due to its simplicity and ease of application. To make the same control robust in nature so that it becomes independent of parameter variations as well as the problems of undershoot and overshoot at the starting time of the response, a pre-compensation using FL is used to the reference signal. As a result, depending upon the value of speed error ($\omega_{re}$) and change in speed error ($\Delta\omega_{re}$), the FL control produces a signal (u), which may be positive or negative in value. The algebraic addition of the FL controller output (u) with the reference speed ($\omega_r^*$) produces the pre-compensated reference speed ($\omega_{r1}^*$) to be used as reference speed in the remaining control action of PI controller. Such a phenomenon of pre-compensation eliminates the possible disadvantages in the normal PI speed controller and introduces robustness to the control system [21].
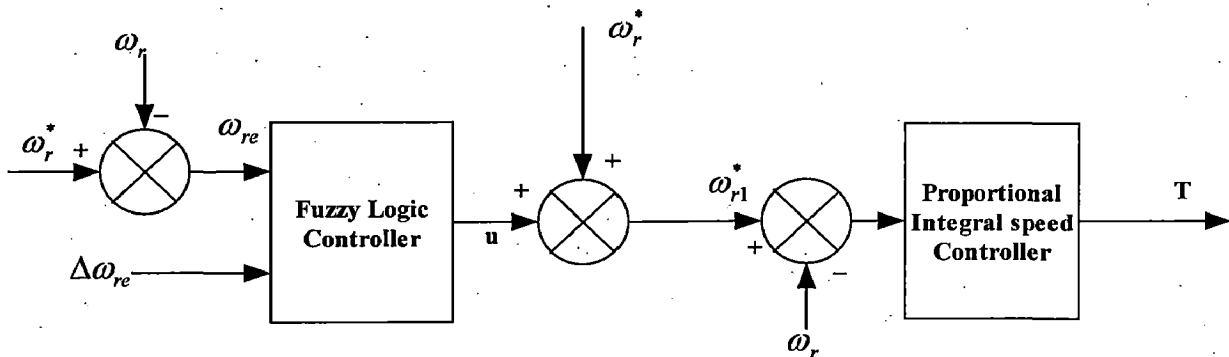


Fig.4.7 Schematic Block diagram of Fuzzy Pre-compensated Proportional Integral (FPPI) speed controller

Fig.4.7 shows the schematic block diagram of FPPI speed controller. The fuzzy rules are stated in table.4.4. The control algorithm process takes place as follows:

(1) At first speed error ($\omega_{re}$) and change of speed error ($\Delta\omega_{re}$) calculated.

(2) After proper scaling these two signals are given to the FL controller, and the output of the FL controller after proper scaling (u) is algebraically added with the reference speed signal($\omega_r^*$) to generate pre-compensated reference speed signal ($\omega_{r1}^*$).

(3) The pre-compensated reference speed signal ($\omega_{r1}^*$) is used as reference speed in PI speed controller.

|  | E | | | | | | |
|---|---|---|---|---|---|---|---|
|  |  | NB | NM | NS | ZE | PS | PM | PB |
| ΔE | NB | NB | NB | NM | NM | NS | NS | ZE |
| | NM | NB | NB | NM | NS | NS | ZE | PS |
| | NS | NB | NB | NS | NS | ZE | PS | PM |
| | ZE | NB | NM | NS | ZE | PS | PM | PB |
| | PS | NM | NS | ZE | PS | PS | PB | PB |
| | PM | NS | ZE | PS | PS | PM | PB | PB |
| | PB | ZE | PS | PS | PM | PM | PB | PB |

Fig.4.4 Logic rules for Fuzzy Logic Controller used for Pre-compensation

## 4.1.2 Limiter:

When the drive operates in the transient conditions such as starting, reversing or load application, the speed controller output (T) is very high value to achieve the steady state condition of the drive as fast as possible. As a result, the controller output signal (T) may become quite high and in some cases it may become higher than the breakdown torque of the motor. Such a situation may be rather dangerous for the motor and may take the drive in to instability, in order to avoid such situations; it becomes very much necessary to apply a certain limit on the output of the speed controller. The output of the speed controller after this limiter is considered as the reference torque (T*) to the vector controller and used to obtain the value of stator current torque component. As a result, the limit on the torque also ensures over current protection to the drive. Whenever reference speed changes or there is an application of load torque on the shaft, the speed controller output is limited to a maximum permissible value (T*). Therefore, the limiter on the speed controller output provides an inherent stability to the closed loop speed control system.

## 4.1.3 Vector Controller:

The output of the speed controller after limiting is taken as the reference torque (T*). When we divide the reference torque with torque constant we will get the torque

component ($i_{qs}^*$) and the flux component ($i_{ds}^*$) of the stator current is always zero for PMSM Drive to avoid the demagnetization. With these two components we can calculate the reference currents $i_{as}$, $i_{bs}$ and $i_{cs}$.

### 4.1.4 Pulse Width Modulated (PWM) Current Controller:

In order to operate the three-phase PMSM into vector controlled mode, sensed three phase stator currents ($i_{as}$, $i_{bs}$ and $i_{cs}$) are to be controlled close to the three phase reference currents ($i_{as}^*$, $i_{bs}^*$ and $i_{cs}^*$). Such a control technique to control the two sets of three phase currents is called current control. PWM current control is one of the current control techniques wherein the switching frequency can be kept constant. The error between the reference three-phase currents and the sensed three phase currents are calculated and the set of current error are amplified with proportional controller and the resulting output is taken as modulating signals which are compared with a carrier triangular wave of required frequency ($f_s$) [6]. For a given phase, the instant at which the modulating switching signal and the triangular carrier wave intersect each other is the instant at which signal for that respective phase changes its logical value between switch off and switch on. The switch on or switch off PWM logic generated for all the three phases are given to the gate driver of MOSFET of VSI.

### 4.1.5 Voltage Source Inverter (VSI):

The three-phase voltage source inverter (VSI) comprises of a bridge configuration of six MOSFET switches with respective free wheeling diodes. The pulses coming from the PWM current controller is fed to this VSI. With this, we can obtain variable voltages with variable frequencies for the permanent magnet synchronous motor, which is operated in vector-controlled mode of operation.

The ac output of the VSI is dependent upon the combination of the switching functions $SF_a$, $SF_b$ and $SF_c$ received from the sinusoidal PWM current controller. Therefore, the magnitude of the three phase voltages can be mathematically expressed as:

$$V_{as} = V_{dc}(2SF_a - SF_b - SF_c)/3$$

$$V_{bs} = V_{dc}(-SF_a + 2SF_b - SF_c)/3$$

$$V_{cs} = V_{dc}(-SF_a - SF_b + 2SF_c)/3$$

Where $V_{as}, V_{bs}$ and $V_{cs}$ are the per phase PWM voltages respectively. $SF_a, SF_b$ and $SF_c$ are the switching functions for phase a, b and c respectively.

## 4.2 IMPLEMENTATION OF SPEED CONTROLLERS IN MATLAB ENVIRONMENT

The simulation model has been developed in MATLAB environment along with simulink and Power System Block set (PSB) tool boxes for simulating response of vector controlled permanent magnet synchronous motor drive under different operating conditions such as starting, speed reversal and load perturbation.
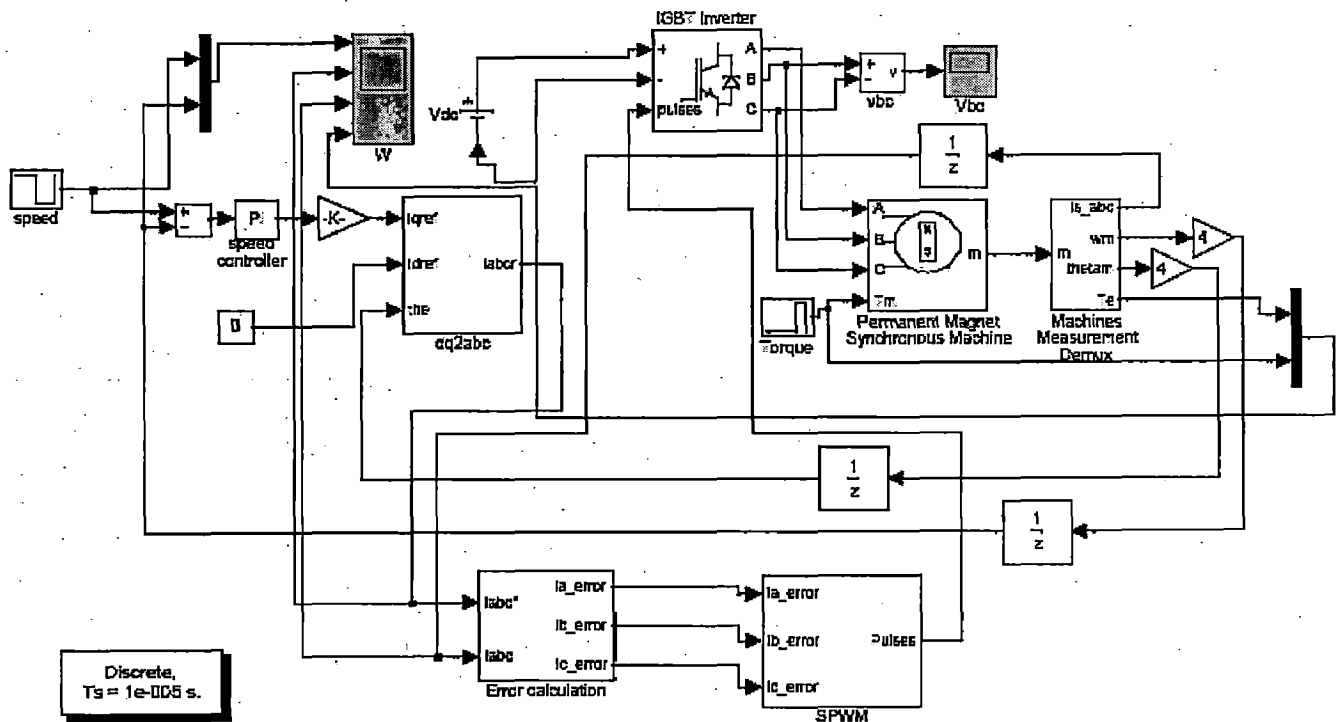


Fig.4.8. Vector controlled permanent magnet synchronous motor drive (VCPMSMD) simulation diagram in MATLAB using simulink power system block set

The main function of speed controller block is to provide a reference torque for the vector controller. Fig.4.9 shows the simulink model diagram of the PI speed controller in discrete time frame. The basic operating equations have been stated in section 4.1.1.1. As seen in figure, using the proportional and integral gain parameters namely, $K_p$ and $K_i$

respectively along with the limiter. The rated torque can be calculated according to the motor rating. The time delay instant $(n-1)^{th}$ instants is achieved by using the delay block.

Fig.4.10 shows the simulink model block diagram for the FL speed controller. The two inputs namely, speed error and change in speed error are properly scaled and fed to the FL controller. The output of the dufuzzification block is again scaled and limited to give the reference torque for the vector controller.
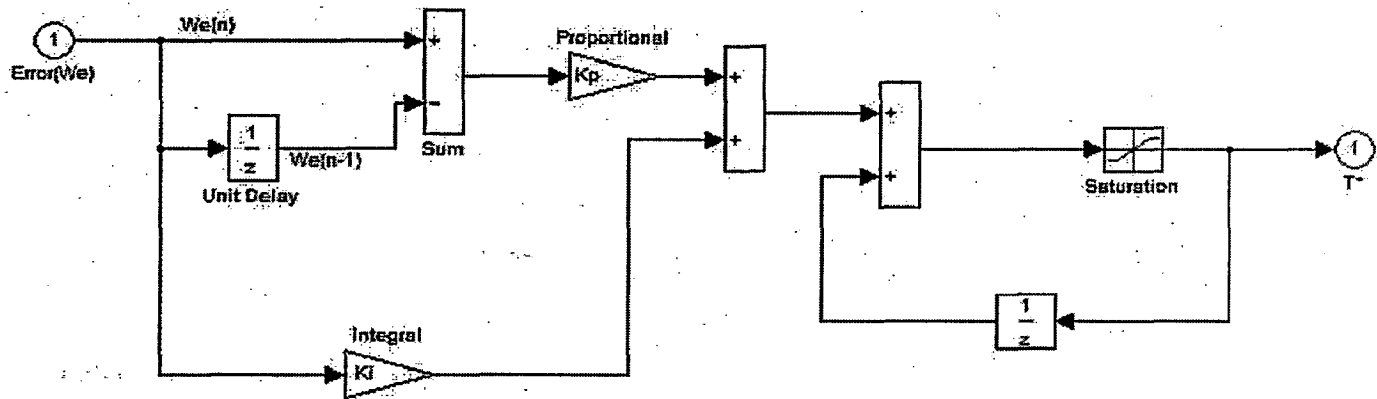


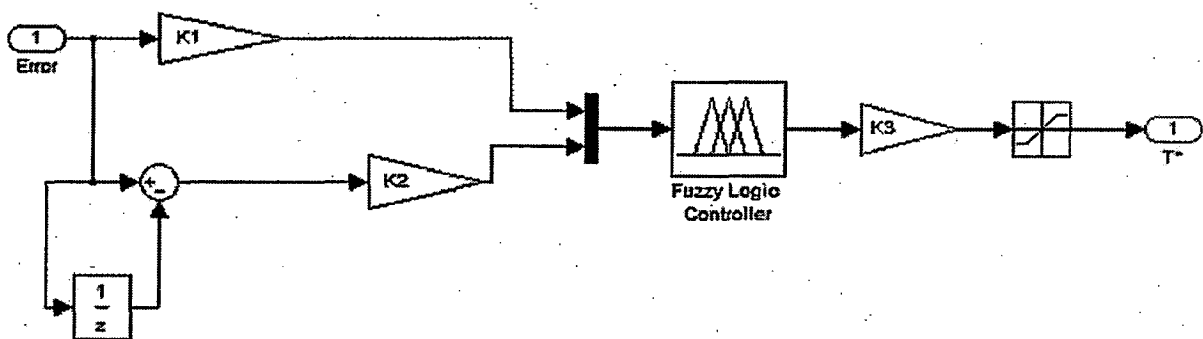Fig.4.9. MATLAB model for Proportional Integral (PI) speed controller



Fig.4.10 MATLAB model for Fuzzy Logic (FL) Speed Controller

Fig.4.11 shows the simulink model block diagram for the hybrid speed controller. This controller combines the outputs of FL and PI speed controllers respectively as a weighted sum. Ta, Tb, Tc and Td denote the hybrid controller outputs corresponding to the speed error. The decision switch decides which option to be transmitted out of the speed controller depending upon the speed error pu value.

Fig.4.12 shows the simulink model block diagram for the FPPI speed controller. The FL controller produces the modified reference speed signal, from which a speed error is calculated, which is fed to the PI speed controller as the reference speed signal.
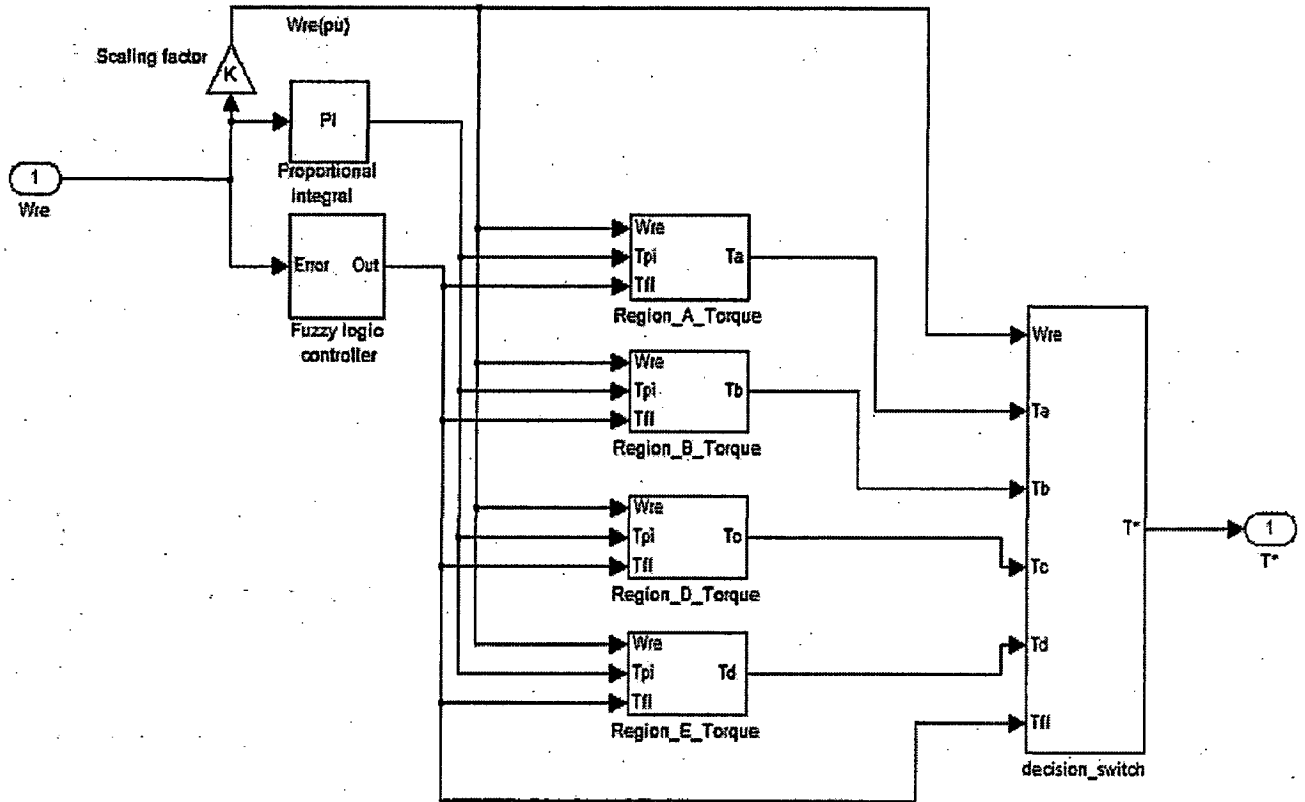


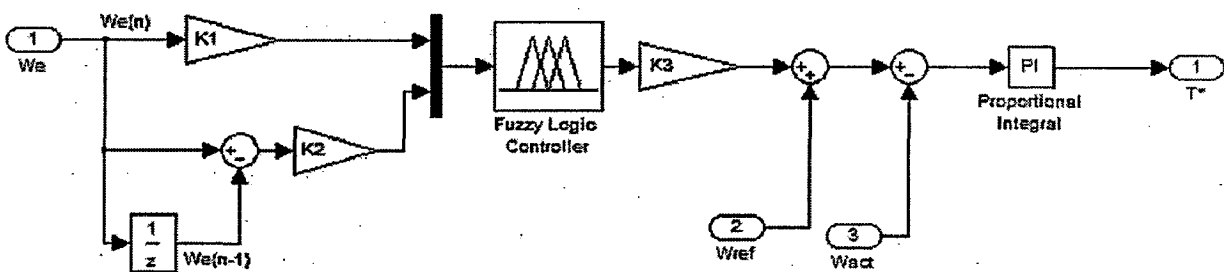Fig.4.11. MATLAB Model for Hybrid speed controller



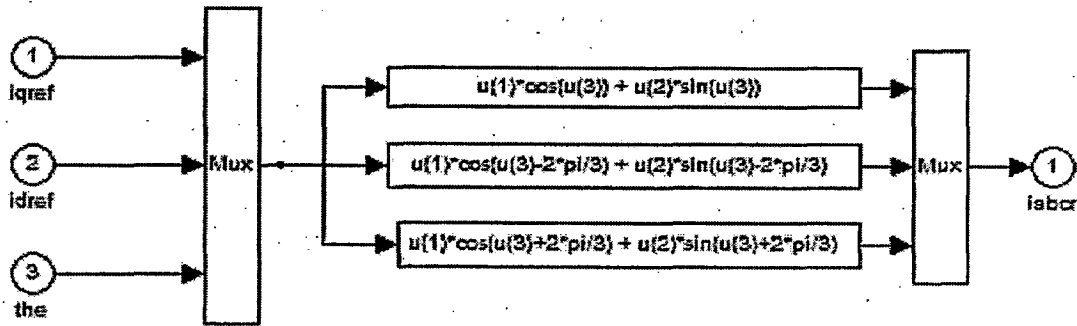Fig.4.12 MATLAB Model for FPPI speed controller

35

Fig.4.13 MATLAB model for conversion of DQ reference current signals to ABC reference current signals

## 4.3 Sensorless vector control of PMSM:

Vector control of PMSM drive requires the knowledge of rotor position and speed. Vector control of PMSM employing position and speed sensors are already discussed in section 4.2. To reduce total hardware complexity and costs, to increase the mechanical robustness and reliability of the drive, to reduce the maintenance requirements and to have noise immunity it is desirable to eliminate these sensors in vector-controlled drives.

The basic control schematic diagram is shown in fig.4.14 two phase currents and voltages constitute the inputs to the electrical rotor position and speed estimator. The error between the reference speed ($\omega_r^*$) and the estimated rotor speed ($\omega_r$) and the error is processed in the speed controller. A limit is kept on the output of the speed controller depending on the maximum permissible torque developed by the motor. The output of the speed controller after limiting is considered as the reference torque ($T^*$). By dividing the reference torque with the torque constant we obtain the torque-producing component of the stator current ($i_{qs}^*$) and the flux component ($i_{ds}^*$) of the stator current is always zero for PMSM Drive to avoid the demagnetization and these two components are converted into the reference currents $i_{as}^*, i_{bs}^*$ and $i_{cs}^*$ .For current control of VSI fed vector controlled PMSM, the reference currents ($i_{as}^*, i_{bs}^*$ and $i_{cs}^*$) and sensed winding currents ($i_{as}, i_{bs}$ and $i_{cs}$) are fed into the Pulse Width Modulated (PWM) current controller. A triangular carrier wave form is generated at the required switching frequency ($f_s$). The point of

intersection of the triangular carrier wave and the modulating signals acts as the point of state changeover for the PWM signals, which are fed to the driver circuit of the MOSFET of VSI feeding PMSM.
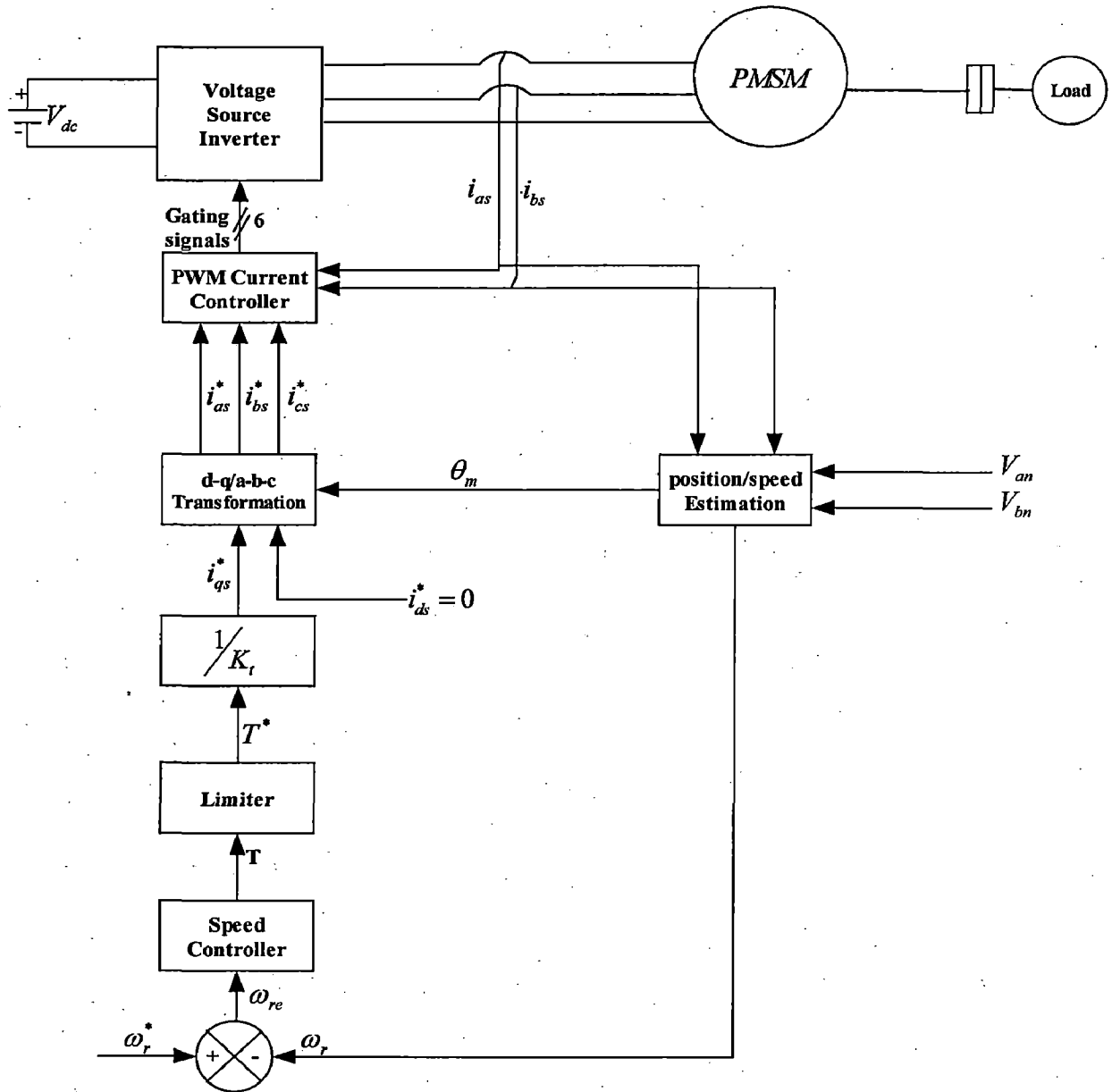


Fig 4.14 Block diagram of sensorless vector controlled PM synchronous motor drive

### 4.3.1 Flux and speed estimation using monitored stator voltages/currents:

Here we are using a simple (open-loop flux estimation) position-sensorless control system for the vector control of a PMSM (with sinusoidal back e.m.f.) supplied by a current-controlled PWM voltage source inverter. The goal is to control the phase angles of the stator currents to maintain near unity power factor over a wide range of speed and torque. For this purpose, the monitored stator voltages and currents are used to estimate the position of the stator flux-linkage space vector through which the phase angles of the stator currents can be controlled.

Open-loop flux estimators can be used in a wide range of a.c. drive applications, including induction motor drives. Such an estimator will yield the angle of the stator flux-linkage space vector with respect to the real axis of the stator reference frame ($\rho_s$), together with the modulus of the flux space vector. These quantities are shown in fig.4.15 In general, for synchronous machine in the steady state, the first time derivative of this angle gives exactly the rotor speed, $\omega_r = d\rho_s/dt$. However, in the transient state, in a drive where there is a change in the reference electromagnetic, the stator flux-linkage space vector moves relative to the rotor (to produce a new torque level), and this influences the rotor speed. This effect can be neglected if the rate of change of the electromagnetic torque is limited [17].

In general, the angle between the stator-current space vector and stator flux-linkage space vector is not $90^0$, but if the stator power factor is to be unity, then the stator-current space vector should lead the stator flux-linkage space vector by $90^0$, and this case is shown in fig.4.15
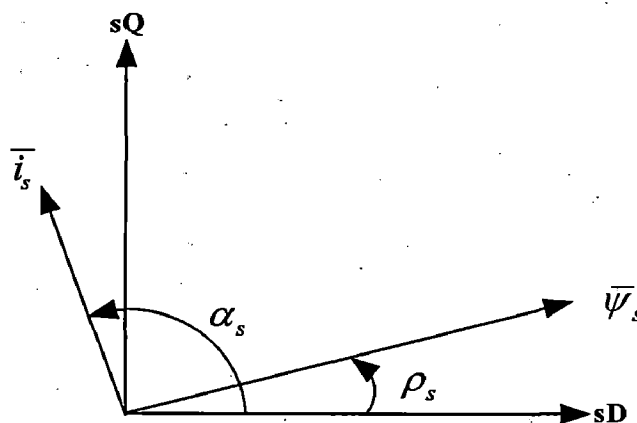


Fig.4.15 Stator current and flux linkage space vector

Open-loop flux estimation [1]:

In general, the stator-flux space vector can be obtained by integration of the terminal voltage minus the stator ohmic drop

$$\overline{\varphi}_s = \int \left( \overline{V}_s - R_s \overline{i}_s \right) dt.$$

Thus the following direct- and quadrature- axis stator flux-linkage components in the stator reference frame are obtained (by considering $\overline{V}_s = V_{sD} + jV_{sQ}$, $\overline{i}_s = i_{sD} + ji_{sQ}$ and $\overline{\psi}_s = \psi_{sD} + j\psi_{sQ}$):

$$\psi_{sD} = \int \left( V_{sD} - R_s i_{sD} \right) dt, \qquad (4.1)$$

$$\psi_{sQ} = \int \left( V_{sQ} - R_s i_{sQ} \right) dt. \qquad (4.2)$$

d-axis,q-axis fluxes are calculated in MATLAB simulink environment as shown in fig.4.16.
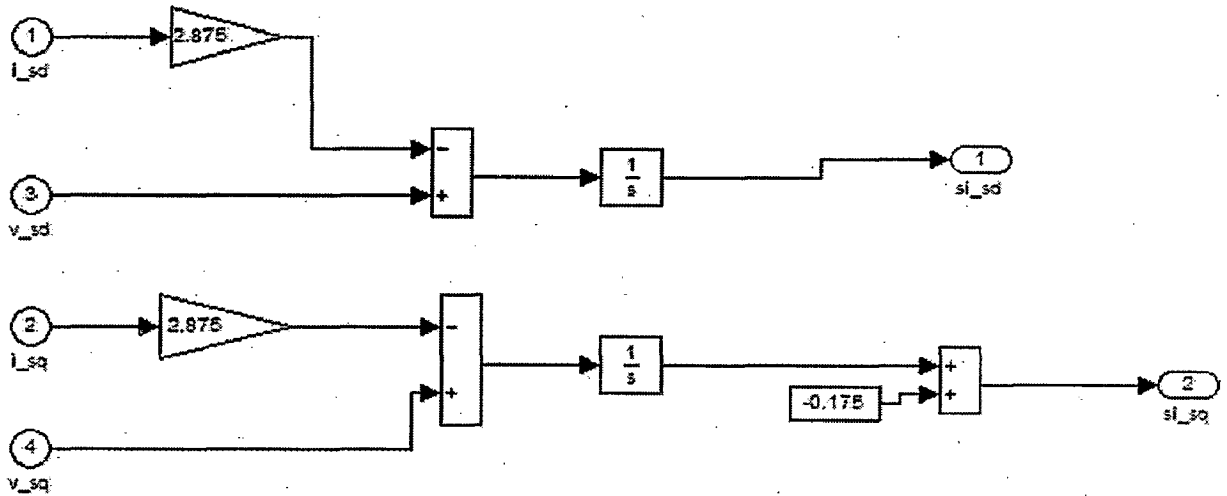


Fig.4.16 MATLAB simulink model for flux estimation of PMSM

Equations 4.1, 4.2 contain the two-axis stator voltages and currents. These can be obtained from the measured line voltages and currents as follows:

$$V_{sD} = \frac{1}{3} \left( V_{BA} - V_{AC} \right)$$

$$V_{sQ} = -\left( \frac{1}{\sqrt{3}} \right) \left( V_{AC} + V_{BA} \right)$$

$$i_{sD} = i_{sA}$$

39

$$i_{sQ} = \left(\frac{1}{\sqrt{3}}\right)(i_{sA} + 2i_{sB})$$

The angle of the stator flux-linkage space vector (which is also shown in fig.4.15) can be obtained from the two-axis stator flux-linkage components as

$$\rho_s = \tan^{-1}\left(\psi_{sQ}/\psi_{sD}\right) \tag{4.3}$$

It is important to note that the performance of a PMSM drive using eqn.4.3 depends greatly on the accuracy of the estimated stator flux-linkage components and these depend on the accuracy of the monitored voltages and currents.

For the synchronous machine, the first derivative of the angle $\rho_s$ is equal to the rotor

speed, $$\qquad \omega_r = \frac{d\rho_s}{dt}$$

And in the speed control loop of the permanent-magnet synchronous motor drive, this relationship can be directly utilized. The estimation of the rotor speed based on the derivative of the position of the stator flux-linkage space vector can be slightly modified, by considering that the analytical differentiation $d\rho_s/dt$, where $\rho_s = \tan^{-1}\left(\psi_{sQ}/\psi_{sD}\right)$, gives

$$\omega_r = \frac{\psi_{sD}\dfrac{d\psi_{sQ}}{dt} - \psi_{sQ}\dfrac{d\psi_{sD}}{dt}}{\psi_{sD}^2 + \psi_{sQ}^2} \tag{4.4}$$
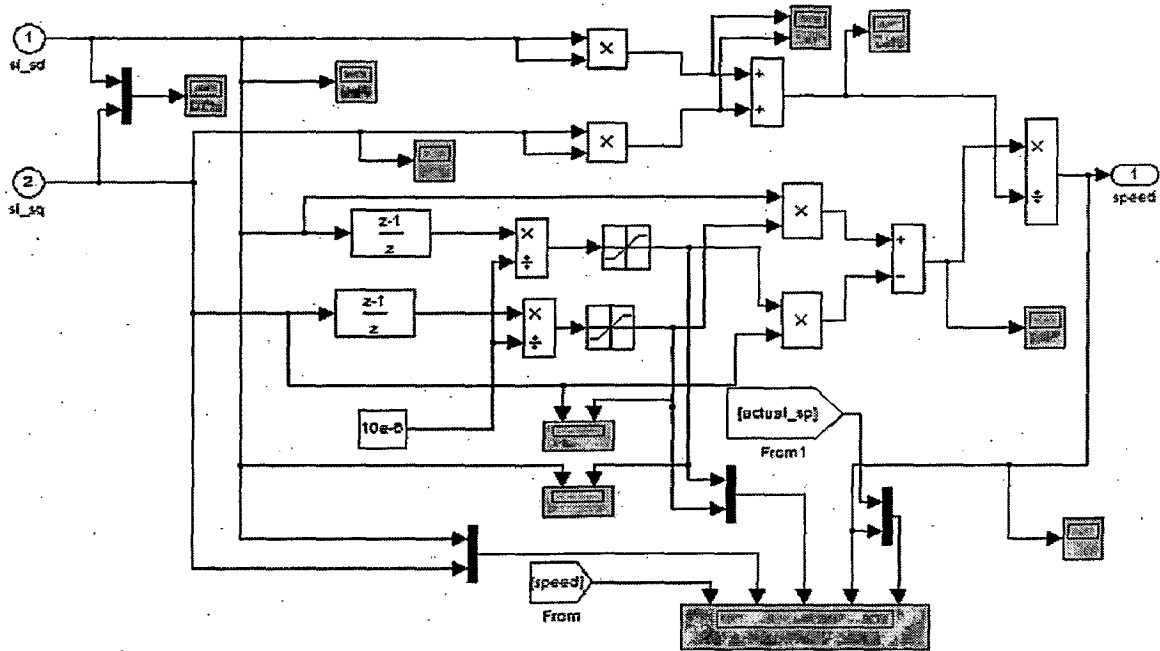
And it is implemented in MATLAB as shown in fig.4.17.

Fig.4.17 MATLAB Simulink model for speed estimation of PMSM drive

# Hardware Implementation

## 5.1 Introduction:

The widely used controlled inverter shown in Fig.5.1, known as the three-phase PWM voltage source inverter (VSI) offers many good features such as very low distortion in voltages and currents on the ac side and the dc side, minimum component count, minimum voltage and current stresses in the components, bi-directional power flow capability, power factor correction and dc voltage regulation capabilities, high power density and high efficiency.

However, it suffers from high switching losses which are aggravated by the reverse recovery characteristics of the diodes. This limits the maximum switching frequency for a given power rating and increases the overall electromagnetic interference (EMI). This in turn prevents any further reduction in size of the filter reactive components and limits the converter bandwidth.

In order to alleviate the switching loss and the reverse recovery problem, some soft-switching techniques, snubbing circuits and gate signal shaping circuits must be used.

## 5.2 Applications of Inverters:

AC/DC power converters/inverters are extensively used in various applications like power supplies, dc motor drives, front-end converters in adjustable-speed ac drives, slip power recovery control of induction motors, HVDC transmission, SMPSs, UPSs, utility interface with non-conventional energy sources such as solar PVs, wind, etc., in process technology like welding, power supplies for telecommunications systems, aerospace, military environment and so on.

Nowadays more and more applications require that the front AC-to-DC converters have both rectifying and regenerating abilities with fast response to improve the dynamic performance of the whole system. A better solution is to use pulse width modulated (PWM) AC-to-DC voltage source converters or current controlled rectifiers (CCR's) which have the merits of nearly sinusoidal input current, good power factor and regeneration ability.

## 5.3 Classification of Inverters:

Inverters can be classified as voltage source inverters (VSI) and current source inverters (CSI). A voltage source inverter is fed by a stiff dc voltage, whereas a current source inverter is fed by a stiff current source. A voltage source can be converted to a current source by connecting a series inductance and then varying the voltage to obtain the desired current.

A VSI can also be operated in current-controlled mode, and similarly a CSI can also be operated in the voltage control mode. The inverters are used in variable frequency ac motor drives, uninterrupted power supplies, induction heating, static VAR compensators, etc.
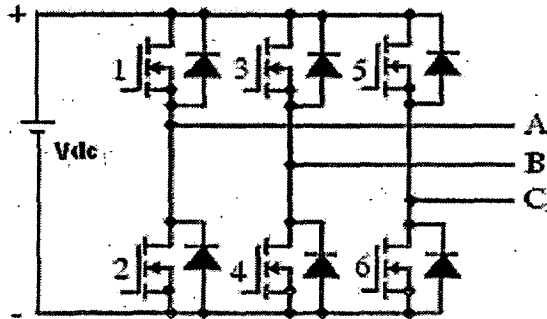
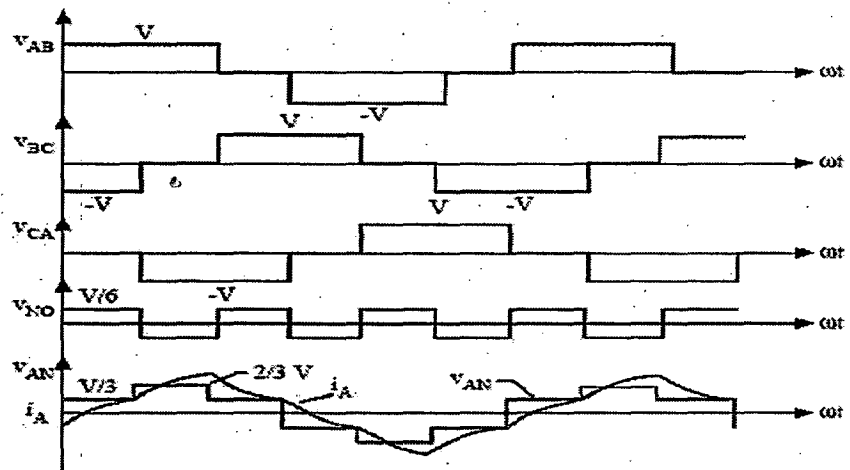Fig 5.1 Three phase voltage source inverter configuration

Fig 5.2 Three phase square wave inverter waveforms

43

## 5.4 Voltage Source Inverter (VSI):

A three-phase voltage source inverter configuration is shown in Fig.5.1; The VSIs are controlled either in square-wave mode or in pulse width-modulated (PWM) mode. In square-wave mode, the frequency of the output voltage is controlled within the inverter, the devices being used to switch the output circuit between the plus and minus bus. Each device conducts for 180 degrees, and each of the outputs is displaced 120 degrees to generate a six-step waveform, as shown in Fig 5.2. The amplitude of the output voltage is controlled by varying the dc link voltage. This is done by varying the firing angle of the MOSFETs of the three-phase bridge converter at the input [4]. The square-wave-type VSI is not suitable if the dc source is a battery. The six-step output voltage is rich in harmonics and thus needs heavy filtering.

In PWM inverters, the output voltage and frequency are controlled within the inverter by varying the width of the output pulses. Hence at the front end, instead of a phase-controlled MOSFET converter, a diode bridge rectifier can be used. A very popular method of controlling the voltage and frequency is by sinusoidal pulse width modulation. In this method, a high-frequency triangle carrier wave is compared with a three-phase sinusoidal waveform, as shown in Fig 5.3. The power devices in each phase are switched on at the intersection of sine and triangle waves. The amplitude and frequency of the output voltage are varied, respectively, by varying the amplitude and frequency of the reference sine waves. The ratio of the amplitude of the sine wave to the amplitude of the carrier wave is called the *modulation index [6]*.

The harmonic components in a PWM wave are easily filtered because they are shifted to a higher-frequency region. It is desirable to have a high ratio of carrier frequency to fundamental frequency to reduce the harmonics of lower-frequency components. There are several other PWM techniques mentioned in the literature. The most notable ones are selected harmonic elimination, hysteresis controller, and space vector PWM technique.

In inverters, if SCRs are used as power switching devices, an external forced commutation circuit has to be used to turn off the devices. Now, with the availability of MOSFETs above 1000-A, 1000-V ratings and high frequency, they are being used in applications up to 300-kW motor drives. Above this power rating, GTOs are generally

used. Power Darlington transistors, which are available up to 800 A, 1200 V, could also be used for inverter applications.
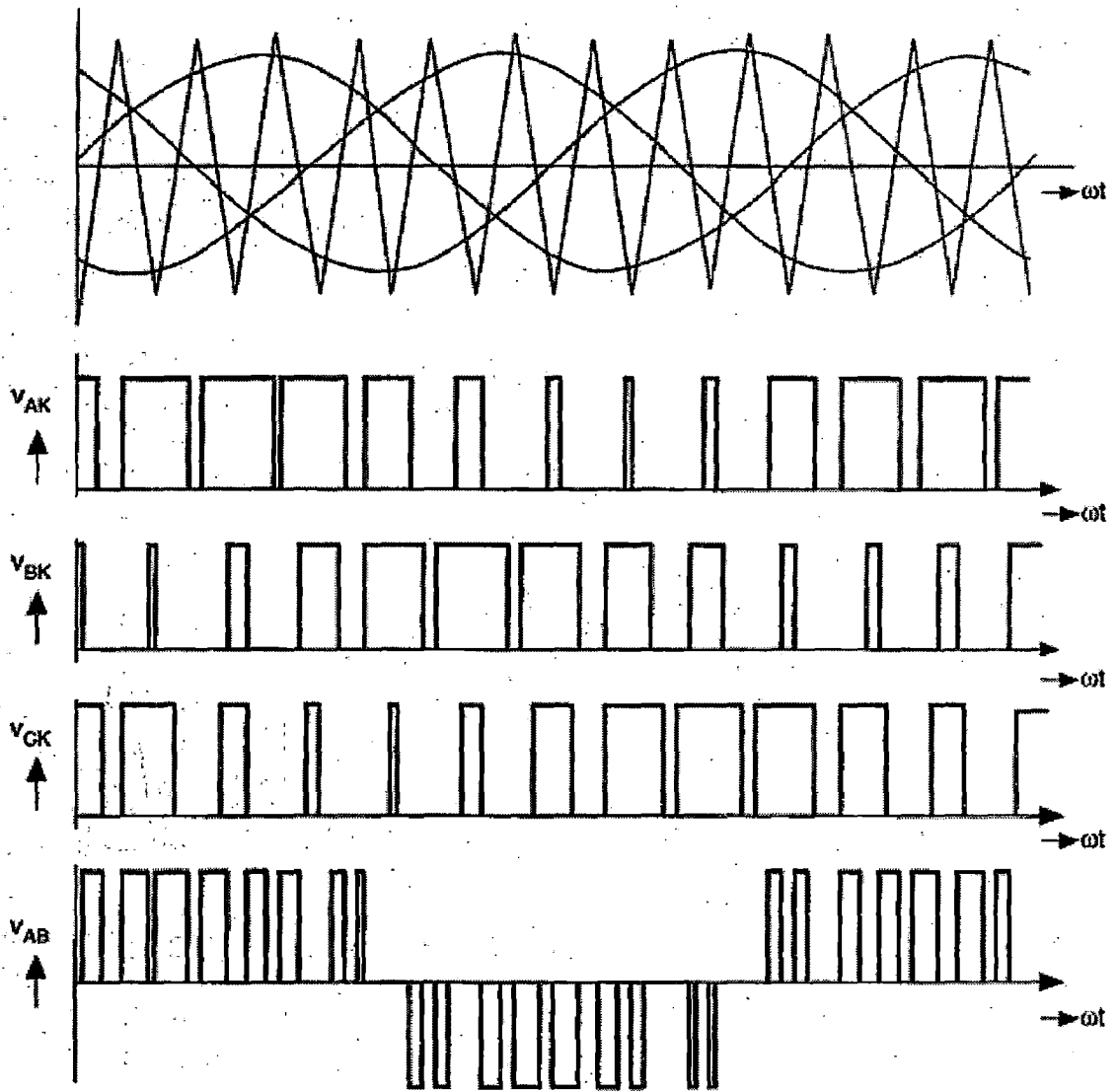


Fig.5.3 Three phase sinusoidal PWM waveforms

## 5.4.1 Metal Oxide Semiconductor Field Effect Transistor (MOSFET):

A power MOSFET has three terminals called drain, source and gate in place of the corresponding terminals collector, emitter and base for BJT. The circuit symbol of power MOSFET is as shown in fig 5.4. Here arrow indicates the direction of electron flow. A

BJT is a current controlled device where as power MOSFET is a voltage-controlled device. As its operation depends upon the flow of majority carriers only, MOSFET is a unipolar device. The control signal or base current in BJT is much larger than the control signal required in a MOSFET. This is because of the fact that gate circuit impedance in MOSFET is extremely high, of the order of $10^9$ ohm. This large impedance permits the MOSFET gate to be driven directly from microelectronic circuit. BJT is suffers from second breakdown voltage where as MOSFET is free from this problem. Power MOSFETs are now finding increasing applications in low power high frequency applications (up to 100 KHz). Power MOSFET conduction conduction is due to majority carriers; there fore time delays caused by removal or recombination of minority carriers are eliminated. Thus power MOSFET can work at switching frequencies in the megahertz range.
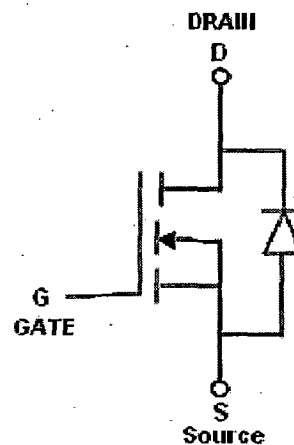
DRAIN
D

G
GATE

S
Source

Fig.5.4 MOSFET Circuit Symbol

**5.4.2 Designing of VSI:**

**5.4.2.1 Power Supply Circuits:**

DC regulated power supplies (+12v, -12v, +5v) are required for providing biasing to various transistors, IC's etc. The circuit diagram for various dc regulated power supplies are shown in fig 5.5; in it the single phase ac voltage is stepped down to 12V and then rectified using a diode bridge rectifier. A capacitor of 1000µf, 50volts is connected at the output of the bridge rectifier for smoothening out the ripples in the rectified DC regulated

46

voltages. IC voltage regulators are used for regulating the voltages on load also. Different IC voltage regulator that are used are; 7812 for +12V, 7912 for -12V and 7805 for +5V. A capacitor of 100µf, 25V capacitor is connected at the output of the IC voltage regulator of each supply for obtaining the constant and ripple free DC voltage.



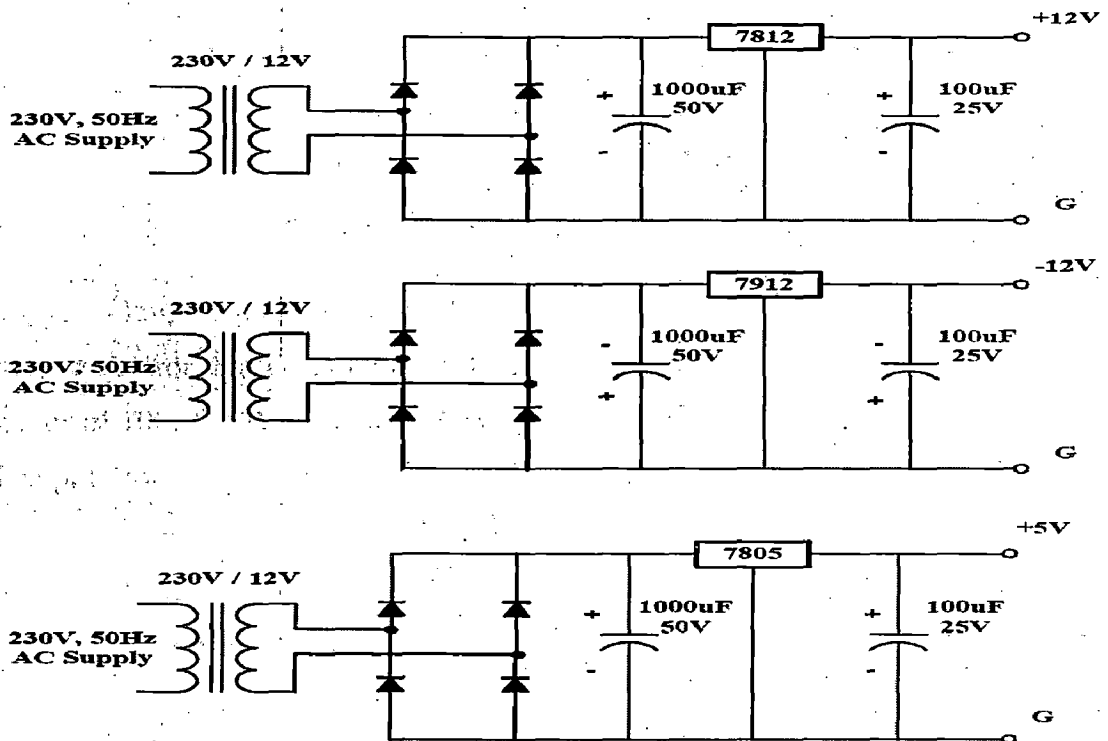Fig.5.5 Circuit Diagrams for IC regulated Power Supplies

| DC VOLTAGE | IC REGULATOR |
|---|---|
| +5V | 7805 |
| +12V | 7812 |
| ±12V | 7812, 7912 |

47

### 5.4.2.2 Pulse Amplification and Isolation Circuit:

The pulse amplification and isolation circuit for MOSFET is shown in figure 5.6. The Opto-coupler (MCT-2E) provides the necessary isolation between the low voltage isolation circuit and high voltage power circuit .The pulse amplification is provided by the output amplifier transistor 2N222.

When the input gating pulse is at +5V level, the transistor saturates, the LED conducts and the light emitted by it falls on the base of phototransistor, thus forming its base drive. The output transistor thus receive no base drive and, therefore remains in cut-off state and a +12 v pulse (amplified) appears across it's collector terminal (w.r.t. ground). When the input gating pulse reaches the ground level (0V), the input switching transistor goes into the cut-off state and LED remains off, thus emitting no light and therefore a photo transistor of the opto-coupler receives no base drive and, therefore remains in cut-off state .A sufficient base drive now applies across the base of the output amplifier transistor .it goes into the saturation state and hence the output falls to ground level. Therefore circuit provides proper amplification and isolation. Further, since slightest spike above 20v can damage the MOSFET, a 12 V Zener diode is connected across the output of isolation circuit. It clamps the triggering voltage at 12.
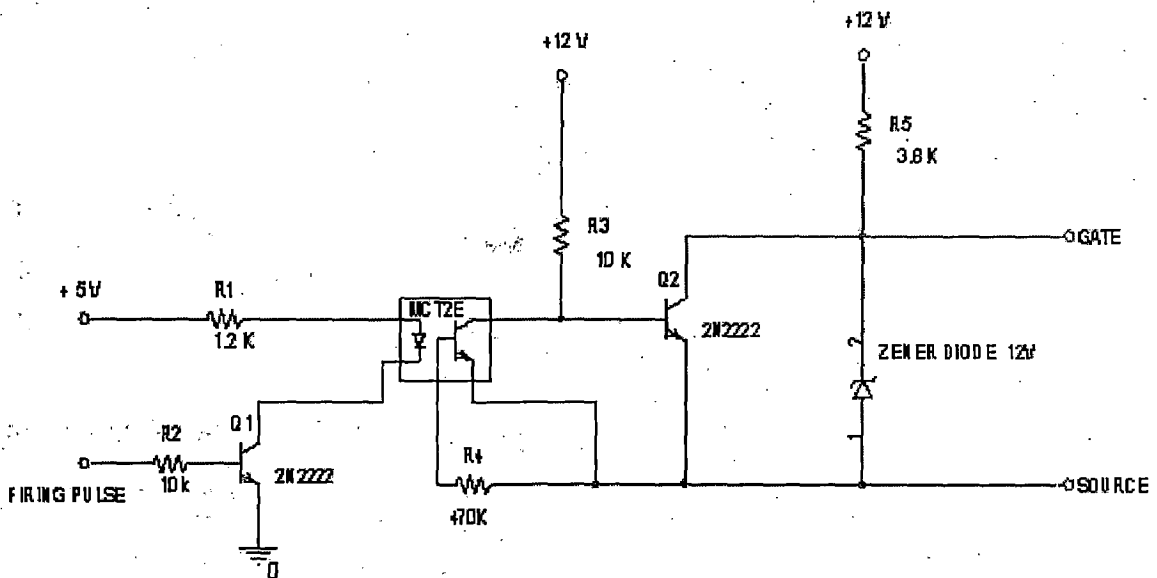


Figure 5.6 Pulse amplification and isolation circuit

### 5.4.2.3 Circuit Protection:

### (A) Snubber Circuit for MOSFET protection:

MOSFETs are used in power electronics application, because of hard switching applications and lower conduction losses. Most of the MOSFETs are used in hard switching applications up to 20 kHz, beyond that switching losses in MOSFETs becomes very significant.

Switching such high currents in short time gives rise to voltage transients that could exceed the rating of MOSFET especially if the bus voltage is close to the MOSFETs rating. Snubbers are therefore needed to protect the switch from transients. Snubber circuit for MOSFETs as shown in Fig.5.7

Snubbers are employed to:

- Limit di/dt or dv/dt.

- Transfer power dissipation from the switch to a resistor.

- Reduce total switched losses.

RCD snubbers are typically used in high current application. The operation of RCD snubber is as fallows: The turn-off makes the voltage zero at the instant the MOSFET turn-off. At turn-off, the device current is transfer through the diode $D_s$ and the voltage across the device builds up. At the turn-on, the capacitor $C_s$ discharges through the resistor $R_s$. The capacitor energy is dissipated in the resistor $R_s$ at turn-on.
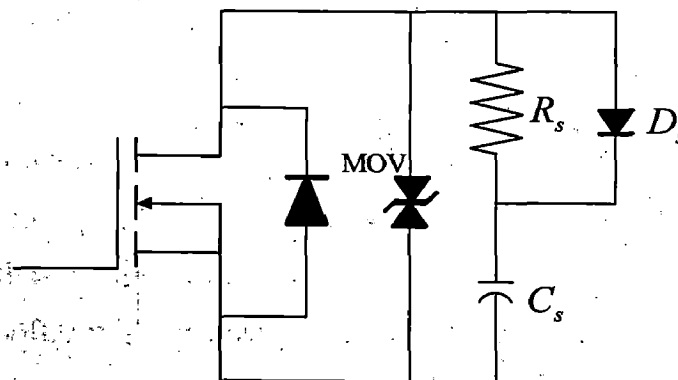


Fig.5.7. Snubber circuit of MOSFET

**(B) Over voltage protection**

An additional protective device Metal-Oxide-Varistor (MOV) is used across each device to provide protection against the over voltages. MOV acts as a back-to-back zener and bypass the transient over voltage across the device. In general the voltage rating of MOV is kept equal are below the rating of MOSFET to protect it from the over voltages.

**(C) Over heating protection**

Due to the ohmic resistance of MOSFET and anti - parallel diode, $I^2 R$ loss takes place as a result of the current conduction, which results the heat generation, thus raising the device temperature, this may be large enough to destroy the device. To keep device temperature within the permissible limits, all MOSFETs are mounted on aluminum heat sink and are then dissipated to the atmosphere.

**(D) Short circuit protection**

The thermal capacity of semiconductor device is small. A surge current due to a short circuit may rise device temperature much above its permissible temperature rise limit which may instantaneously damage the device. Hence, the short circuit protection is provided by fast acting fuses in series with each supply line.
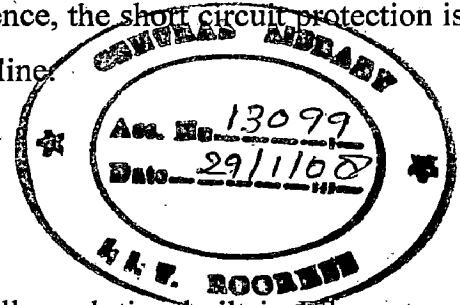
**5.5 I-8438 Embedded Controller**

**5.5.1 Introduction:**

I-8438 is the ICP DAS MATLAB Embedded Controller solution built in Ethernet and series interface with I/O expansion slot for MATLAB development environment. For this application there are over 20 I/O bridges and system-level Simulink blocksets have been developed. By using Simulink development environment and these MATLAB Driver's blocksets, control algorithm can be easily constructed and verified without writing any code. Once the algorithm has been verified, by pressing a build button, we can convert a model to executable code, and download it to controller for test or practical application via RS232 and Ethernet [26].

## 5.5.2 Simulink model with ICPDAS driver:

If the simulation output was satisfied, we can replace the built-in Simulink blocks with the I-8000 driver blocks. To add an I-8000 driver block to the model, follow these steps:

**Step 1:** Insert a SYS_INIT block from the System block library.
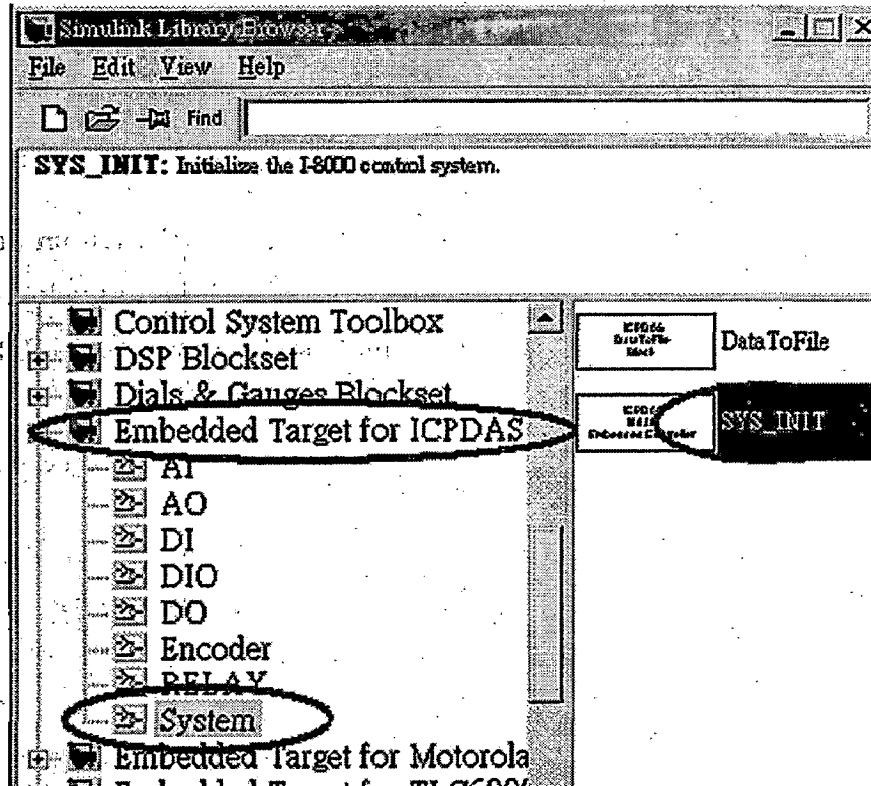


**Step 2:** Double-click on the SYS_INIT block to open the SYS_INIT dialog box. Then select the correct type from the popup menu on the dialog box. Here, we select the type as I8438.

**Step 3:** Connect the blocks (Analog & Digital I/O) where ever we needed in the simulink Block.

### 5.5.3 Build the program by RTW:

In this section, we will discuss how to convert the control model created in the previous section into an .exe file by RTW. To do this, just follow the following steps:

**Step 1:** Open the Simulation Parameters dialog box by choosing *Simulation parameters* from the *Simulation* menu.

**Step 2:** On the dialog box that displays, select Type as *Fixed-step*, Mode as *Single Tasking* in the "Solver options" field.

**Step 3:** Then click the "Real-Time Workshop" tab and the pane changes. On the pane that shows up, select "Target configuration" from the "Category" field. Then click the Browse button to open the "System Target File Browser" window.

**Step 4:** On the System Target File Browser dialog, select the correct system target file from the list and then click the OK button to close the dialog box. Here, we choose I_8438.tlc.
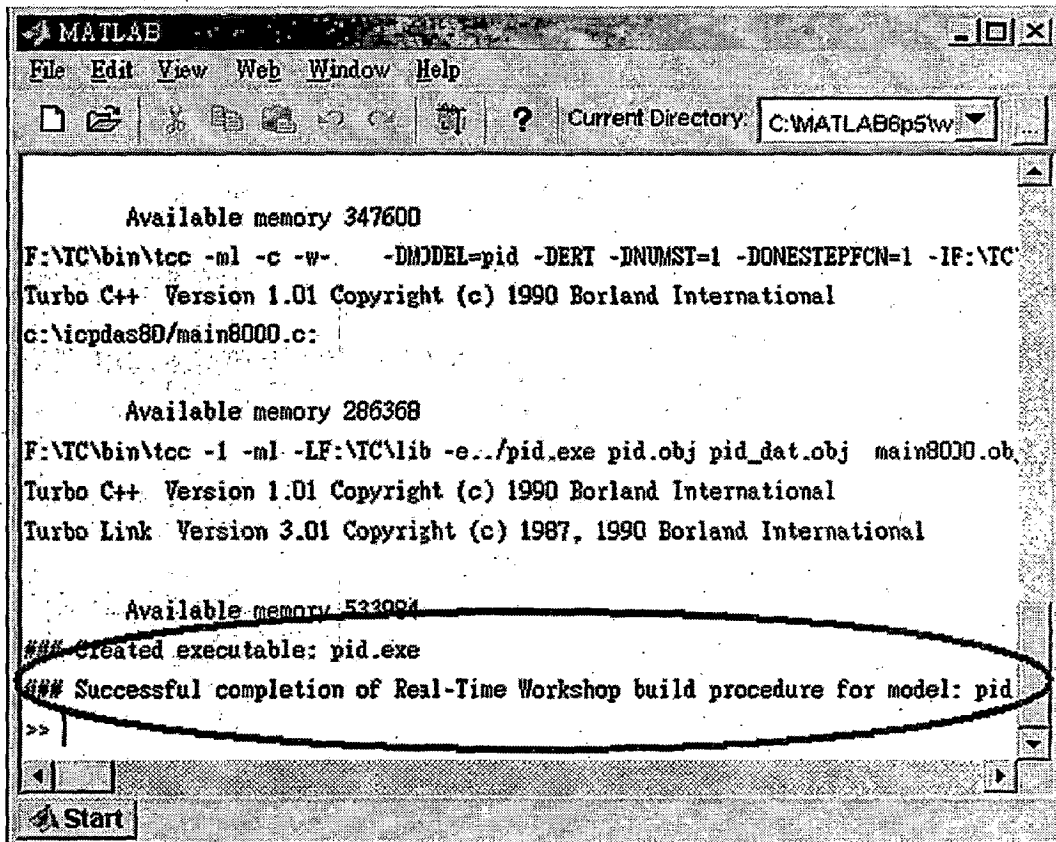
**Step 5:** And select the "ERT code generation options" (for MATLAB 6.1) or "ERT code generation options (1)" (for MATLAB 6.5) in the Category field. Then check the **Terminate function required** and **Single output/update function** options on the pane.

**Step 6:** For MATLAB 6.5, you have to select "ERT code generation options (3)" from the Category field. Then cancel the option **Generate an example main program**.

**Step 7:** When the above steps are done, click the Build button to start the build process. After the process ends successfully, the message in the MATLAB command window looks like as the following figure.

**Note:**

The name of the model cannot be over 4 characters. (This is due to the limitation of Turbo C/C++ Compiler)

```
MATLAB                                                          _ □ ×
File  Edit  View  Web  Window  Help

  □  ☞  |  ✂  🖹  📋  ⟲  ⟳  | 📇 |  ? | Current Directory: C:\MATLAB6p5\w  ▼  ...

         Available memory 347600
F:\TC\bin\tcc -ml -c -w-    -DMODEL=pid -DERT -DNUMST=1 -DONESTEPFCN=1 -IF:\TC
Turbo C++  Version 1.01 Copyright (c) 1990 Borland International
c:\icpdas8D/main8000.c:

         Available memory 286368
F:\TC\bin\tcc -l -ml -LF:\TC\lib -e../pid.exe pid.obj pid_dat.obj  main8000.ob
Turbo C++  Version 1.01 Copyright (c) 1990 Borland International
Turbo Link  Version 3.01 Copyright (c) 1987, 1990 Borland International


         Available memory 533004
### Created executable: pid.exe
### Successful completion of Real-Time Workshop build procedure for model: pid
>>

Start
```

## Program downloading & data uploading:

After the build process is completed, you can download the executable file generated to the I8438 embedded controller in the following way:

Enter **gui8000** at the MATLAB prompt, and the GUI dialog box appears. It provides two communication modes, RS232 and TCP/IP, for us to download application program.
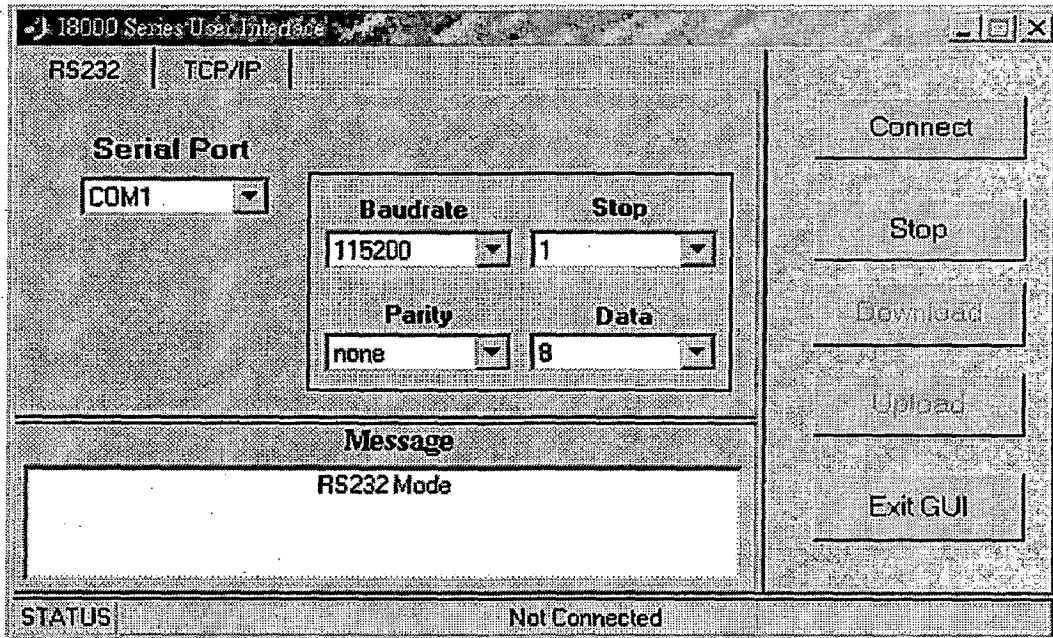
In RS232 mode, follow steps to download the program to the I-8438 target system for application:

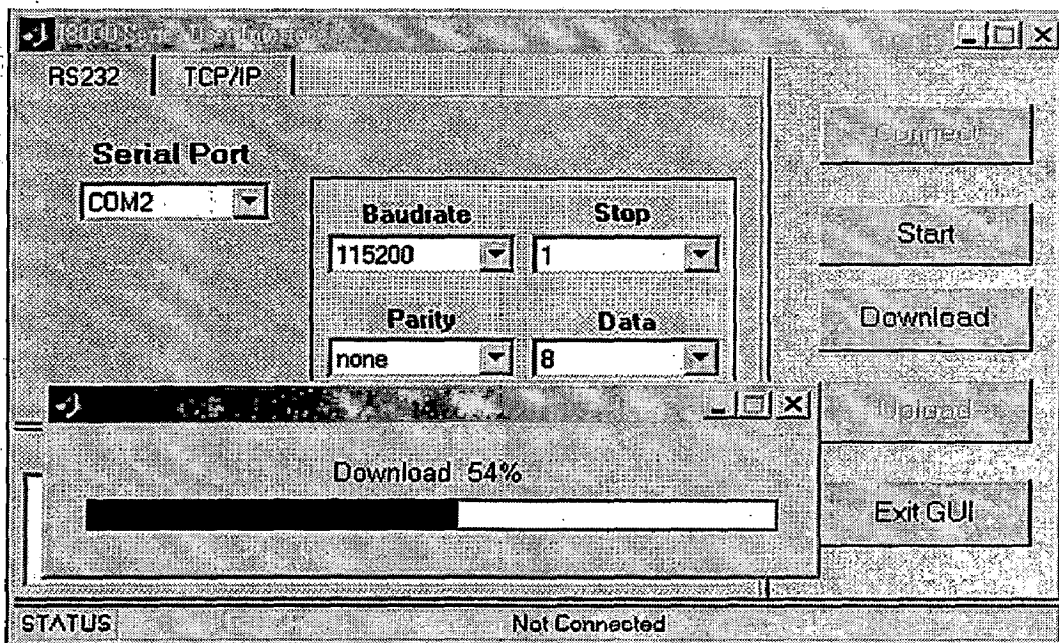**Step 1:** Turn on the I-8438 control system and **set I-8438 control system in OS mode**

**Step 2:** Enter **gui8000** command at the MATLAB prompt and the GUI dialog box appears.

**Step 3:** Select the serial port you use in the PC to connect to the I-8438 control system. Then set *Baud rate, Parity, Data bits, Stop bit* as '115200, none, 8, 1'. The default baud rate of the I-8438 control system is 115200.

**Step 4:** Close 7188xw.exe first and then click the *Connect* button. If the connection is successful, the message, "Connection is established' on the dialog box", will show up.

**Step 5:** Now it's time to download your program. Click the *Download* button and the *Select File to Download* dialog box appears. Select the file you want to download to the I-8438 control system and press the OK button to close the dialog box and then the download process starts.

**Step 6:** On the dialog box that appears, you can see the progress of program downloading. Then you can click the *Start* button to run your control program after the progress of program downloading was finished.

**Step 7:** After we execute the program successfully, then you can click the *Upload* button to collect the data from the I8438 control system, and data will be saved in a file whose name is the filename we assigned in the Data to File dialog box. This data file will be placed in the current working directory. And if we use analog/digital I/O modules the output will be available in that module. This o/p is indicated by the glow of LED's on that corresponding analog/digital I/O module

### 5.5.4 I-8438 Controller Modules:

There are 3 types of modules in 8438 controller. They are:

1. Analog input module (i-8017)
2. Analog output module (i-8024)
3. Digital input/Output module (i-8054)

## 1. Analog input module (I-8017):

### Description:

8-channel Isolated Analog Input Module.

```
     ┌──────┐
     │     0├>
     │     1├>
     │     2├>
     │     3├>
     │     4├>
     │     5├>
     │     6├>
     │     7├>
     └──────┘
      I-8017H
```
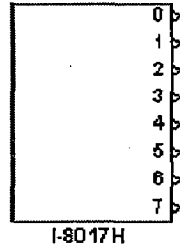
### Driver Block Parameters:

**Channel** - Enter numbers between 0 and 7. This block allows the selection of analog input lines in any order. The number of elements defines the number of analog inputs used. For example, to use the first 8 analog inputs, enter [0 1 2 3 4 5 6 7]

**Voltage range** - TheI-8017H, AI module, provides 4 ranges of the input voltage, and they are +/-10V, +/-5V, +/-2.5V, and +/-1.25V.

**Slot** - The number of the slot where I-8017H module is located. For example, choose 2 from the popup list if you have mounted an I-8017H module on slot 2.

**Type of Value** - Floating or Hex is available. The table below presents the list of ranges of the input voltage.

## 2. Analog output module (I-8024):

### Description:

4-channel Isolated Analog Output Module.

```
     ┌──────┐
   >│0     │
   >│1     │
   >│2     │
   >│3     │
     └──────┘
      I8024
```
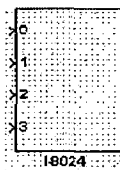
### Driver Block Parameters:

**Output Mode** — *Voltage Out* or *Current Out* is available.

- Voltage Output -> +/-10V
- Current Output -> 0~20mA

**Output channel** - Enter numbers between 0 and 3. This block allows the selection of analog output lines in any order. The number of elements defines the number of analog outputs used. For example, to use the first 4 analog outputs, enter [0 1 2 3]
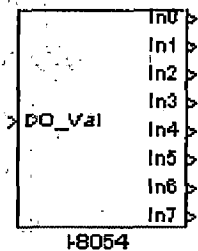
**Gain** - A multiplier. The default value is 1.

**Slot** - The number of the slot where I-8024 module is located. For example, choose 2 from the popup list if you have mounted an I-8024 module on slot 2.

**Type of Value** - Floating or Hex is available. The following table presents the difference between them.

### 3. Digital input/Output module (I-8054):

**Description:**

16-channel Isolated Digital I/O Module.



**Driver Block Parameters:**

**DI Channel** - Enter numbers between 0 and 7. This block allows the selection of digital input lines in any order. The number of elements defines the number of digital inputs used. For example, to use the first 8 digital inputs, enter [0 1 2 3 4 5 6 7]

**Slot** - The number of the slot where I-8054 module is located. For example, choose 2 from the popup list if you have mounted an I-8054 module on slot 2.

Scaling input to output (digital output):

| Block input value | Hardware Output |
|---|---|
| 0 | All channels are off |
| 1 | ch0 is on, others are off |
| 2 | ch1 is on, others are off |
| .... | .... |
| 255 | All channels are on |

## 5.6 Generation PWM Signals by using I-8438 Controller:

Many control strategies are there to control the VSI. But here we are using SPWM .In SPWM, triangular carrier wave of frequency 'fc' is compared with the fundamental frequency 'f' sinusoidal modulating wave, and the points of intersection determine the switching points of power devices.

But i-8438 controller doesn't support continuous waveform blocks like triangular block. So by using discrete blocks we should develop triangular waveform. Then, we compare this triangular signal with sinusoidal waveforms in the dsp controller; this will give 6-pulses available at the Digital o/p module, which are used for switching the IGBTs in the inverter.
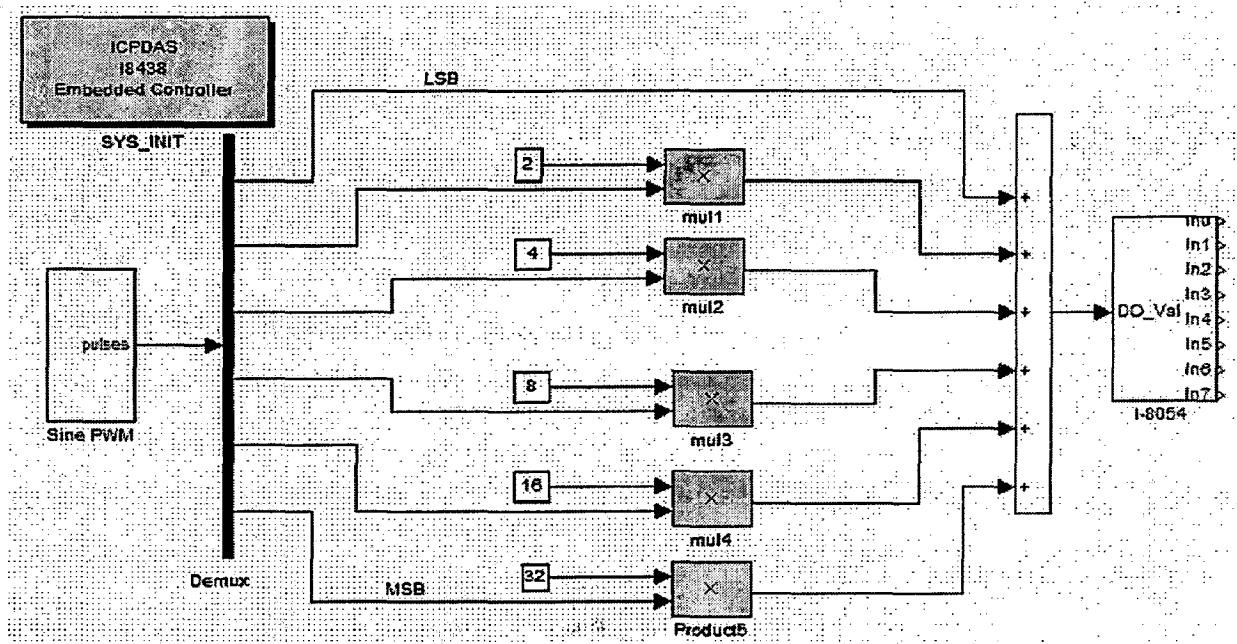
Fig.5.7 Embedded controller based implementation of SPWM technique for VSI

In the above fig.5.7 we obtain 6-pulses from the SPWM block, pulses are represented by 0 or 1. When the pulse is high, it is represented by 1; otherwise it is represented by 0. At first these six pulses i.e. binary values (0's and 1's) are converted in to decimal form then this decimal value is given to the digital o/p module (i-8054) of the controller. This module gives the binary values at the o/p ports (0, 1, 2, 3, 4, and 5) which is equivalent to the i/p decimal number i.e. the o/p of each port represents one pulse. The o/p of six ports represents six pulses.
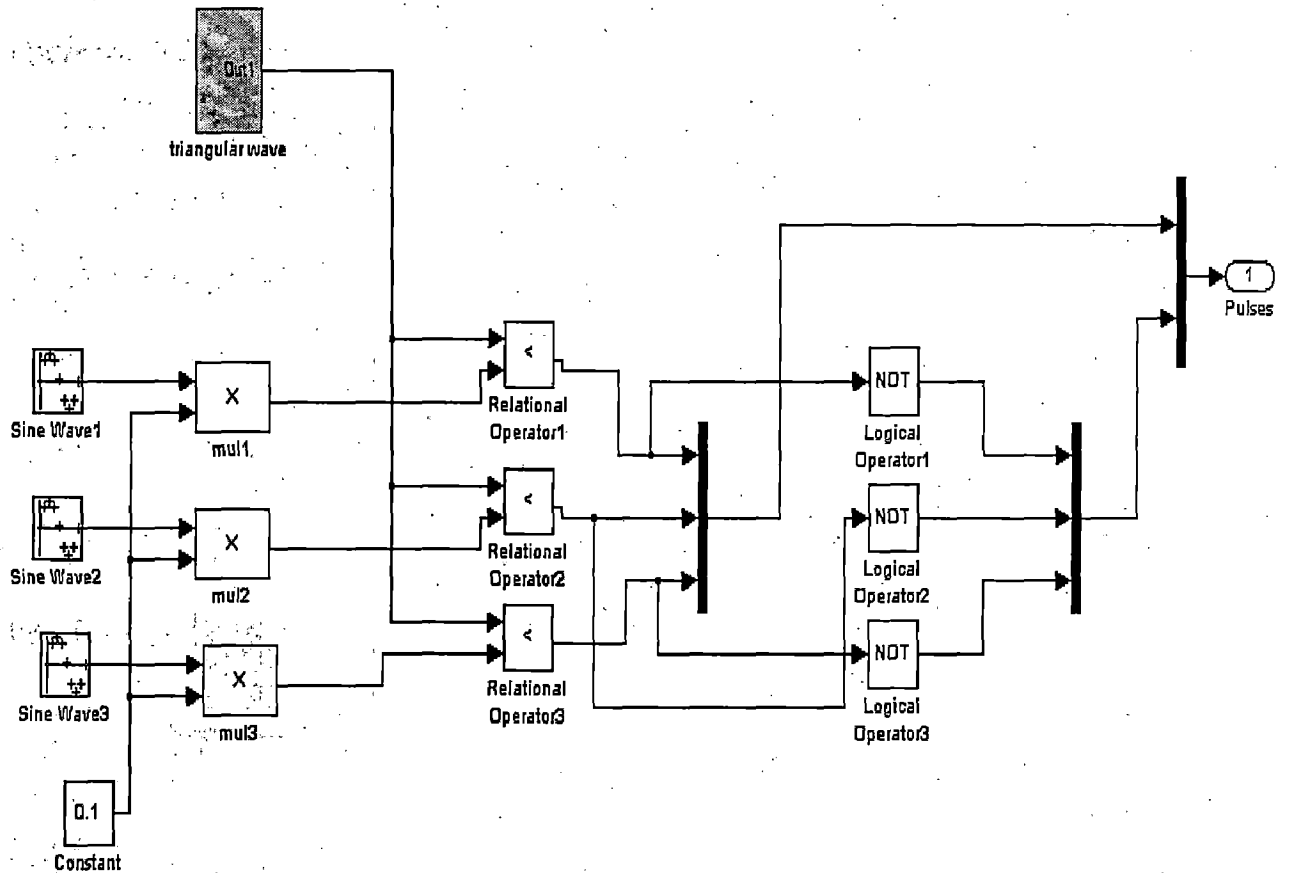
## 5.6.1 MATLAB model:



Fig 5.8 MATLAB model for sinusoidal PWM technique

## 5.6.2 Triangular waveform generation:

I8438 Embedded controller does not support the repeating sequence waves. In order to generate the pulses we have to compare sinusoidal signal with triangular waveform. So we have to generate the triangular waveform. Fig.5.9 shows the MATLAB Simulink model for triangular wave form generator.
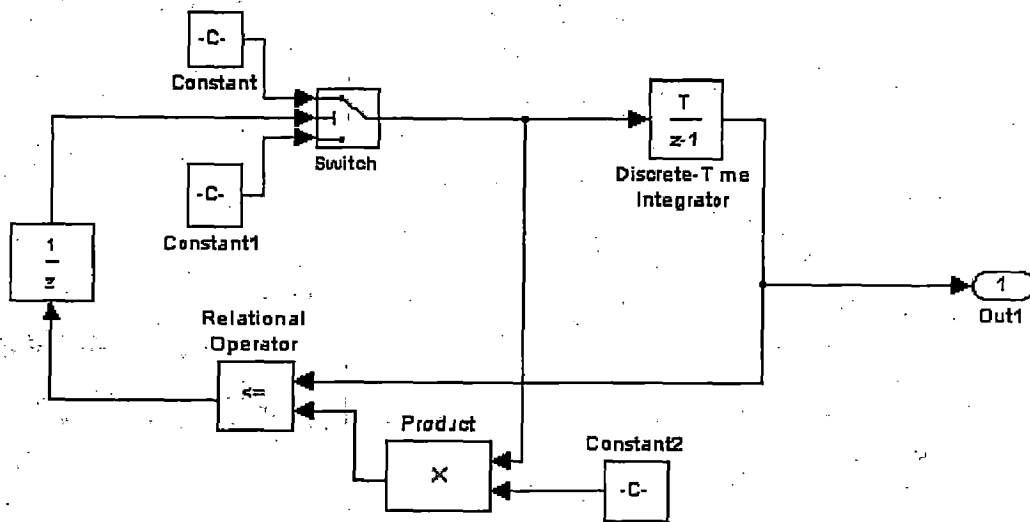
Fig 5.9 MATLAB model for triangular waveform generation

# Results and Discussions

The performance of the vector controlled PMSM drive is simulated under different dynamic conditions such as starting, speed reversal and load perturbation. A set of response comprises reference speed $(\omega_r^*)$, rotor speed $(\omega_r)$ in electrical rad./sec., three phase reference currents($i_{as}^*, i_{bs}^*$ and $i_{cs}^*$), three phase winding currents $(i_{as}, i_{bs}$ and $i_{cs})$ in amperes and the load torque $(T_L)$ and actual torque $(T_e)$ in Nm. The vector controller is realized as a discrete structure in time domain. The performance for starting, speed reversal and load perturbation are shown in figs.5.1-5.8.

## 6.1 Starting Dynamics:

The motor is started at low frequency decided by the controller and finally runs at steady state condition at the set reference value of speed. The reference speed is set at 200 rad./sec. with a torque limit set at twice the rated value so that the starting current is also limited within the twice of the rated current. When the speed error reduce to almost zero the winding current reduces to the no load value. The starting dynamics are shown in Fig.6.1-6.8.

## 6.2 Reversal Dynamics:

The speed reversal dynamics are also shown in fig. 6.1-6.8 while the motor is running at a steady state speed of 200 rad./sec, the reference speed is changed from 200 rad/sec to -200 rad/sec. In response to this change, the control structure is first activated and a large value of the speed error saturates the output of the speed controller. As a result, regenerative braking followed by reverse motoring takes place. Therefore, the controller first reduces the frequency of the stator currents demonstrating the regenerative braking followed by the phase reversal for reverse motoring. As the drive in the same dynamic state just before and after the reversal phenomenon, the steady state values of the inverter currents are observed to be same in either direction of rotation of the motor. However the phase sequence of these currents in two directions will be different.

## 6.3 Load Perturbation:

When the motor is running at steady state speed of 200 rad./sec., a load torque equal to the rated torque of the motor is applied on its shaft. Sudden application of load causes an instantaneous fall in the speed of the motor. In response to the drop in speed, the output of the speed controller responds by increasing the reference torque value $(T^*)$. Therefore, the developed electromagnetic torque of the PMSM increases causing the motor speed to settle to the reference value with the increasing winding currents. An exception of a small amount of steady state speed error persisting in FL speed controller is observed.

When the motor operating at steady state on load, suddenly the load is removed, a small overshoot in the speed of the motor is observed in case of PI, Hybrid and FPPI speed controllers respectively. Therefore the input to these speed controllers become negative causing a reduction in the output of the speed controllers. A change in the developed torque is observed leading to the motor speed to fall down to the reference value. After the load removal the stator currents also settle down to the steady state no load value. In this manner the controller keeps the motor running at a constant speed under load variations.

## 6.4 Comparative study among all the speed controllers:

The simulated results for the 3.5kw and 1.1kw VCPMSMD under different operating conditions namely starting, speed reversal and load perturbation using different speed controllers namely Proportional Integral (PI), Fuzzy, Hybrid and Fuzzy Pre-compensated PI (FPPI) respectively are shown in figs.6.1-6.8.

The following observations are made from these results.

Table 6.1 Comparative performance of different speed controllers for 3.5 kw VCPMSMD

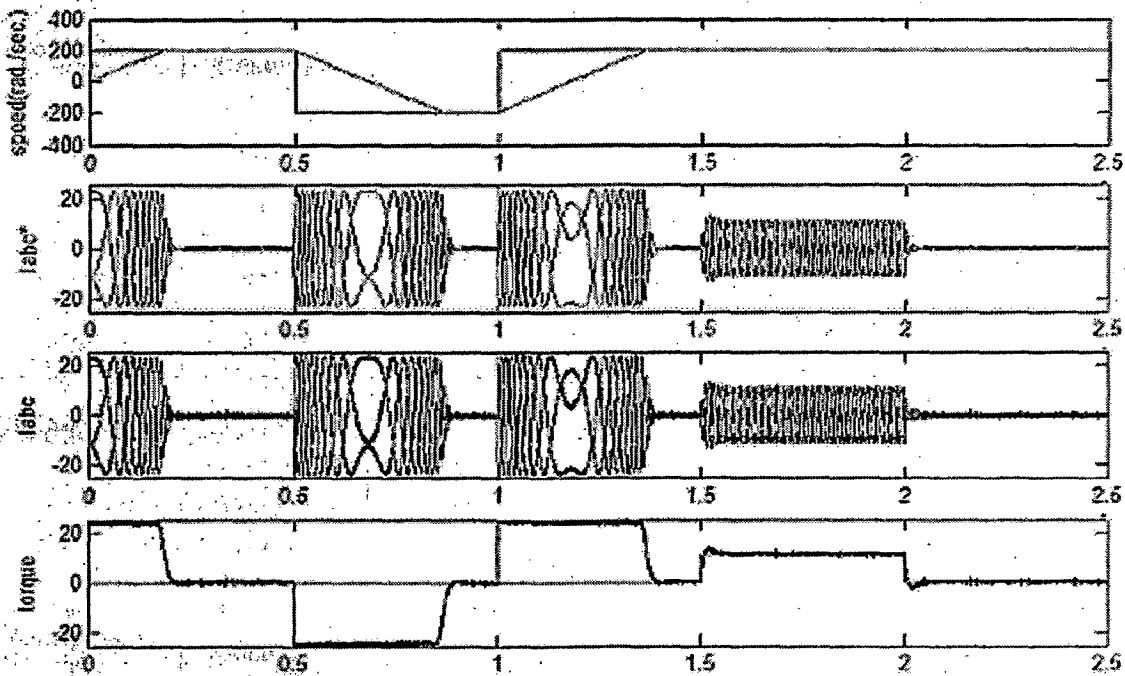| Speed Controller | Starting Time (msecs) | Reversal Time (msecs) | Speed dip on full load application (rad/sec) | speed rise on full load removal (rad/sec) | Steady state speed error on full load (rad/sec) |
|---|---|---|---|---|---|
| PI | 198.51 | 380.12 | 2.21 | 2.33 | 0 |
| FL | 191.01 | 365.21 | 0 | 0 | 1.5 |
| Hybrid | 194.32 | 368.91 | 2.10 | 2.09 | 0 |
| FPPI | 188.50 | 366.52 | 0.61 | 0.58 | 0 |



Fig.6.1 Starting, Speed reversal and load perturbation response of 3.5kw VCPMSMD
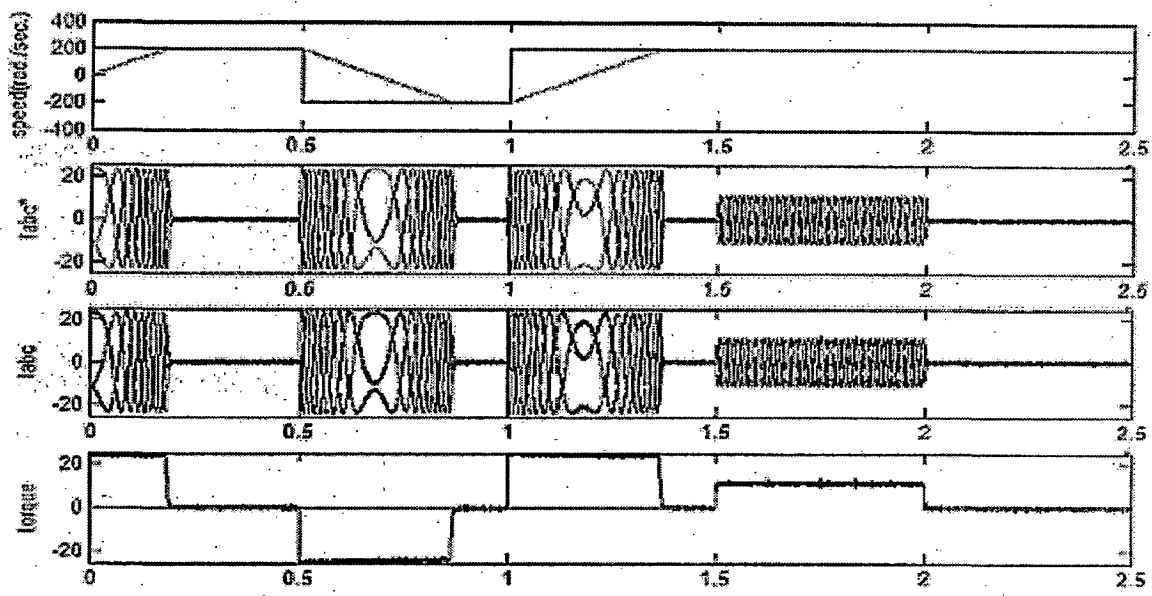System with PI speed controller

Fig.6.2 Starting, Speed reversal and load perturbation response of 3.5kw VCPMSMD System with FL speed controller
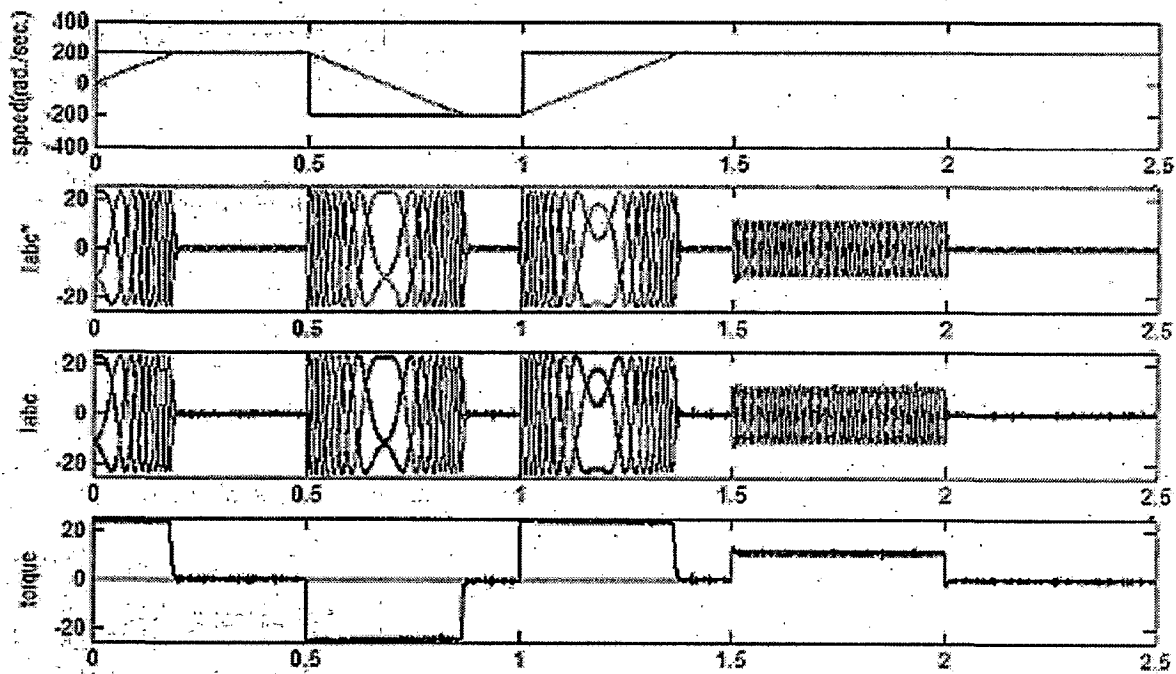


Fig 6.3 Starting, Speed reversal and load perturbation response of 3.5kw VCPMSMD System with Hybrid speed controller
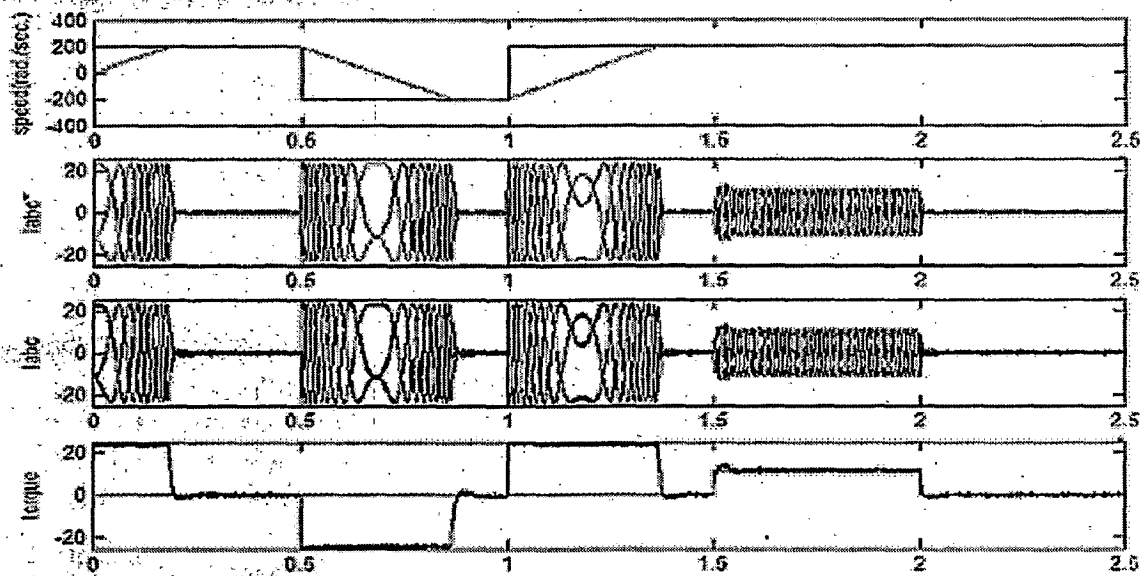
Fig.6.4 Starting, Speed reversal and load perturbation response of 3.5kw VCPMSMD
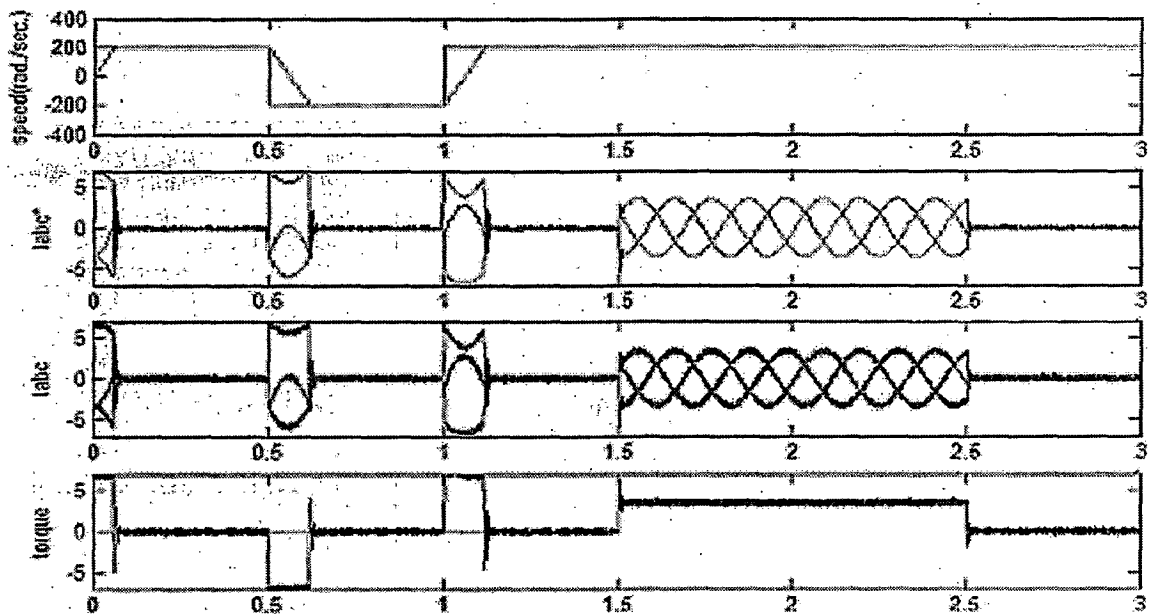System with FPPI speed controller



Fig.6.5. Starting, Speed reversal and load perturbation response of 1.1kw VCPMSMD
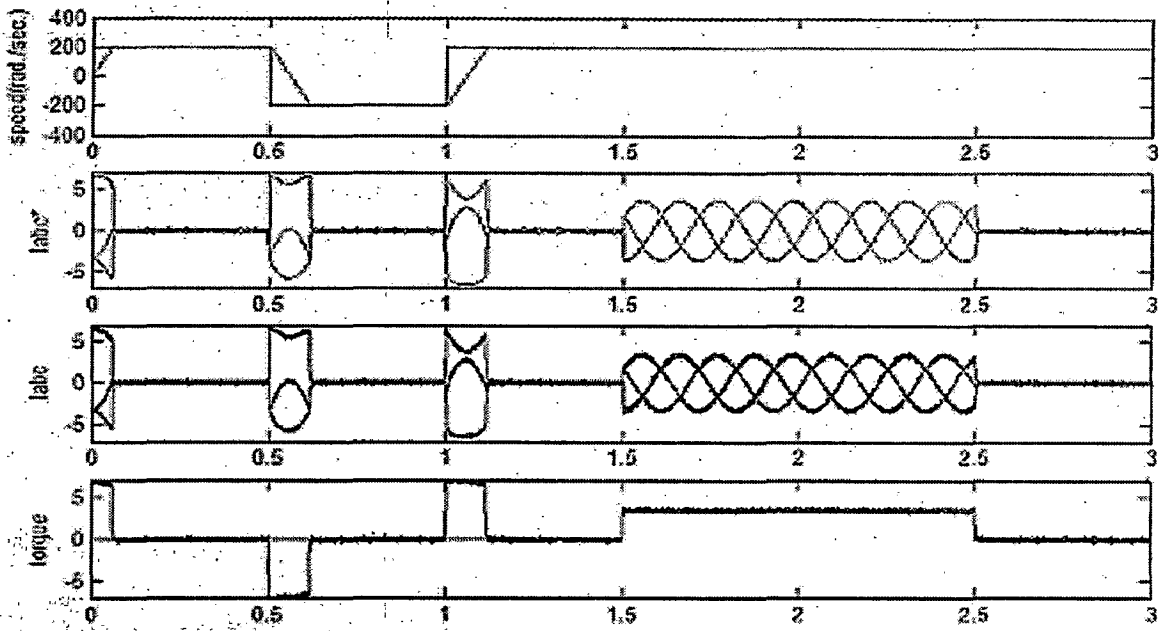System with PI speed controller

Fig.6.6 Starting, Speed reversal and load perturbation response of 1.1kw VCPMSMD
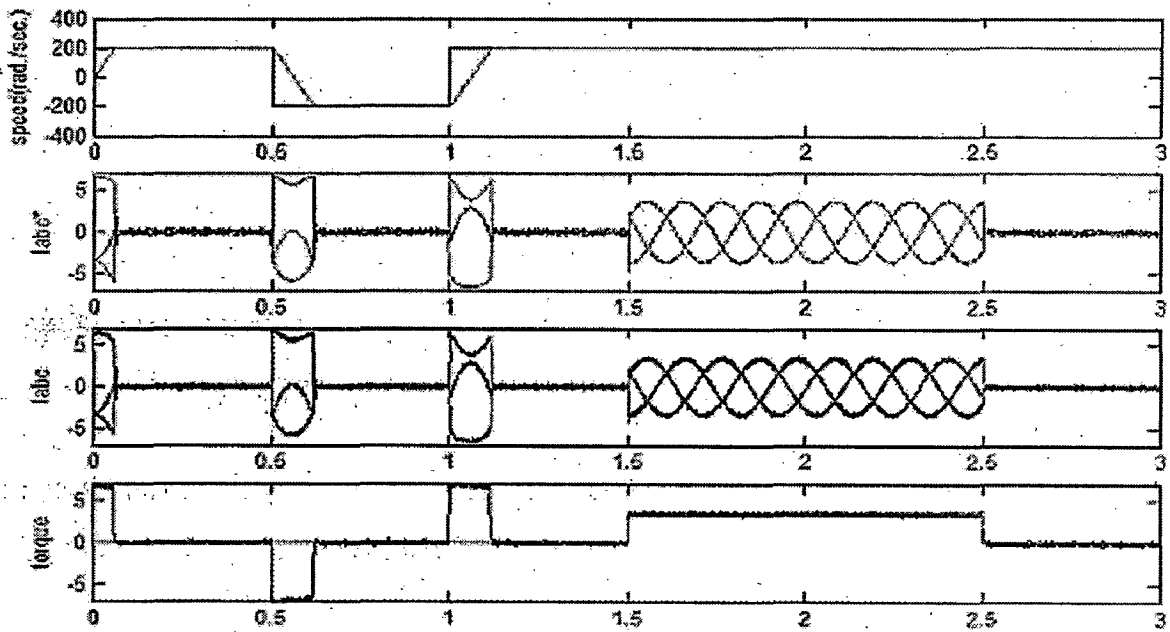System with FL speed controller



Fig.6.7 Starting, Speed reversal and load perturbation response of 1.1kw VCPMSMD
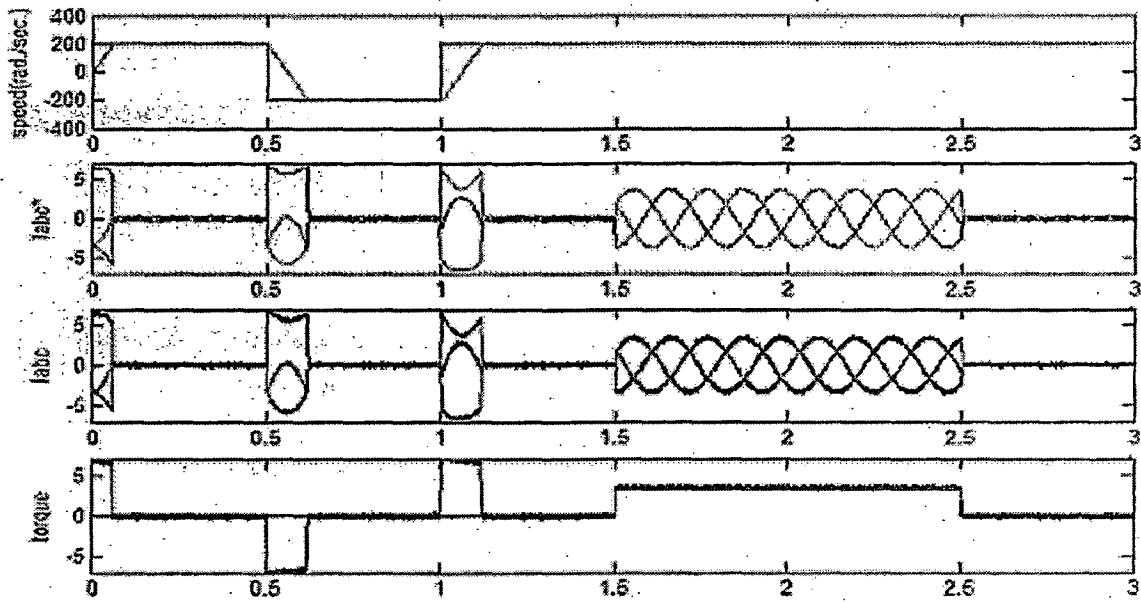System with Hybrid speed controller

Fig 6.8 Starting, Speed reversal and load perturbation response of 1.1kw VCPMSMD System with FPPI speed controller

Table 6.2 Comparative performance of different speed controllers for 1.1kw VCPMSMD

| Speed Controller | Starting Time (msecs) | Reversal Time (msecs) | Speed dip on full load application (rad/sec) | speed rise on full load removal (rad/sec) | Steady state speed error on full load (rad/sec) |
|---|---|---|---|---|---|
| PI | 7.01 | 12.80 | 4.51 | 5.01 | 0 |
| FL | 6.35 | 12.20 | 0 | 0 | 4.10 |
| Hybrid | 6.29 | 11.91 | 3.21 | 3.01 | 0 |
| FPPI | 6.12 | 11.80 | 3.11 | 2.12 | 0 |

When we use PI speed controller small overshoots and under shoots are observed in the response of the VCPMSMD. When PI controller is replaced with FL controller, steady state error on load is observed. In order to take the advantages of PI and FL controllers and to eliminate disadvantages of the individual controller, both the control techniques are combined together as a hybrid speed controller. When the speed error is near to zero, the control is switched over to PI controller therefore eliminating disadvantage of steady state speed error of FL speed controller. When drive speed is away from the reference value, the control is changed over to FL controller, which provides good dynamic response. Instead of solely depending on the speed error, if FL controller is applied to modify the reference speed and the main control action uses PI speed controller then a drastic improvement is observed in the performance of the VCPMSMD system. Such a speed controller is named as Fuzzy Logic Pre-compensated PI (FPPI) speed controller. It can be observed that FPPI speed controller provides a high level of performance of VCPMSMD system during starting, speed reversal and load perturbation for different motors.

Fig. 6.9 shows estimated flux, speed and rotor position without sensors. Noise is coming in speed and flux wave forms when the machine is in dynamic state (when speed rising and falling). The noise is eliminated when the machine is running in steady state.
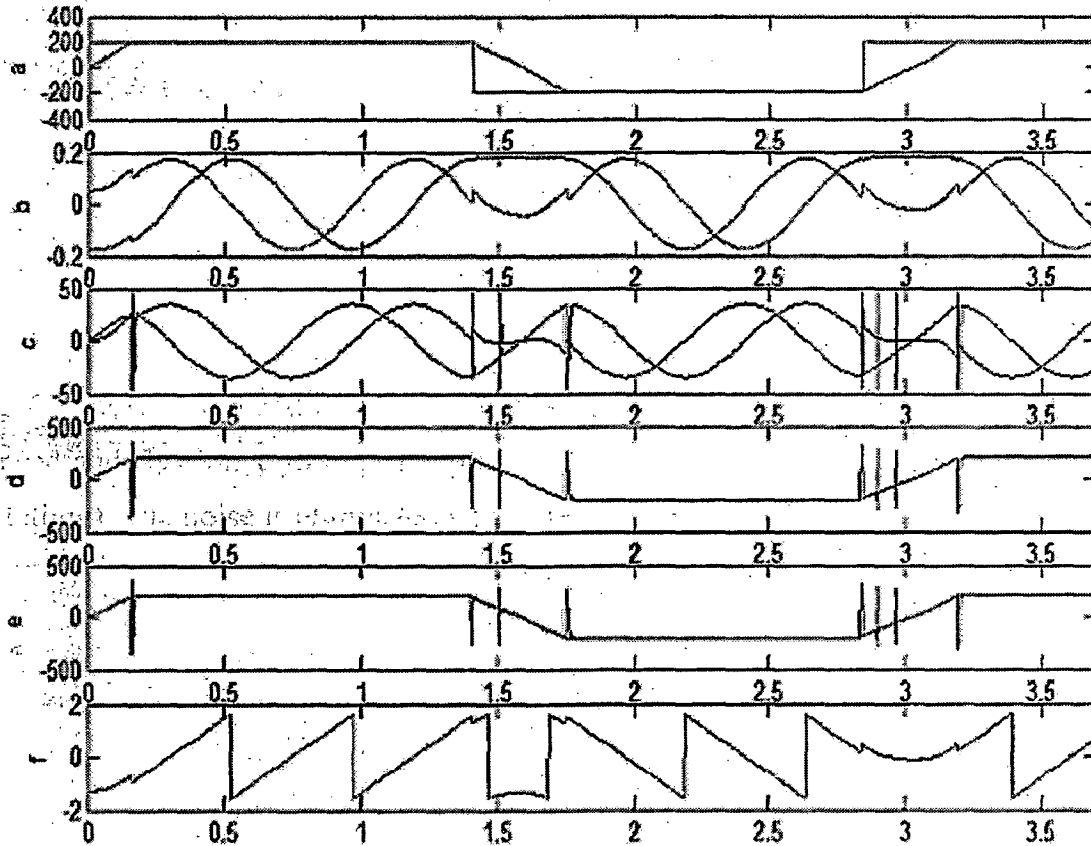


(a) Reference speed, actual speed (rad./sec.)  (b) Flux (d-axis, q-axis) in wb.

(c) Derivative of flux (d-axis, q-axis)  (d) Estimated speed (rad./sec.)

(e) Actual speed, estimated speed (rad./sec.)  (f) Estimated position (rad.)

Fig.6.9 Estimated rotor position, speed and flux of the sensorless control of VCPMSM

Drive

# Conclusion

In this present work, performance of the Vector Controlled Permanent Magnet Synchronous Motor Drive (VCPMSMD) is carried out using different speed controllers under various operating conditions, in MATLAB environment using simulink Power System Block set (PSB) tool boxes. An algorithm for speed estimation has also been developed in order to eliminate the speed sensors in VCPMSMD for reducing the cost and improving the reliability. Sinusoidal pulse width modulation technique is implemented with I-8438 embedded controller.

Mathematical model of the VCPMSMD has been developed in terms of parameters and physical variables of the motor. The performance of VCPMSMD is studied during various operating conditions such as starting, speed reversal and load perturbation. The response of the VCPMSMD system has been simulated in MATLAB environment using simulink and PSB tool boxes. A comparative study of different speed controllers has been carried out for the VCPMSMD system. The comprehensive study of different speed controllers for various operating conditions of VCPMSMD system has shown that the individual speed controllers have their own merits and demerits. Depending on the application, a choice of a particular speed controller may be made. When the requirements are that of simplicity and ease of application the Proportional Integral (PI) controller is a good choice. For better dynamic response without disadvantages such as overshoot and undershoot, the Fuzzy Logic (FL) technique is opted for. The main disadvantage in this FL speed controller operation is the existence of the steady state error on load application. To eliminate such problems and to maintain the high level of performance, the combination of FL and PI is a better option. Such a combination is referred as the Hybrid control. To retain simplicity and ease of application and eliminate the disadvantages such as overshoot and undershoot etc., the reference speed signal is pre-compensated with FL controller. This pre-compensated speed signal is used as reference speed signal to the PI speed controller. Such a combination is known as Fuzzy Pre-compensated Proportional Integral (FPPI) speed controller. Through simulations it

has been confirmed (as per table 6.1 and 6.2) that the choice of FPPI turns out the best among the four considered speed controllers.

We sensed the speed in VCPMSMD by using the speed sensor. The presence of such a speed sensor causes several disadvantages such as system overall cost, hard ware complexity and noise. The speed estimation technique for the elimination for the speed sensor is based on motor currents and voltages in two of the three phases. On the basis of these sensed variables, the speed of the motor is estimated. It has also been confirmed that the estimated motor speed agreed well with the actual motor speed.

With respect to hardware, sinusoidal Pulse width Modulation technique is implemented with I-8438 embedded controller and the modulated pulses have been generated. Although there have been technical limitations in the I-8438 controller the PWM signals up to 300 Hz only could be generated. The operational limitations of I-8438 resulted in non-implementation of the practical controllers and drive.

The future scope is the experimental validation of simulated results by, developing a PMSM drive through a DSP based controller design and using PWM current controlled inverter employing constant frequency triangular carrier of at least 5KHz, in order to obtain the required dynamic response of the drive system.

The best performance indexes are:
1. Zero steady state speed error.
2. Least overshoots in speed on full load removed.
3. Relatively very low speed dip on application of full load.
4. Reversal time approaching the best possible in the case of Fuzzy Logic.
5. FPPI controller gave the minimum starting time out of all the four controllers.

# References

1. Peter Vas, *"Vector control of AC machines,"* Oxford University Press, New York, 1990.

2. T.J.E.Miller, *"Brushless Permanent Magnet and Reluctance Motor Drives,"* Clarendon Press, Oxford Science Publishers, 1993.

3. Bimal K.Bose, *"Power electronics and Variable Frequency Drives-Technology and Applications,"* IEEE Press, 1997.

4. Bimal K.Bose, *"Modern Power Electronics and AC Drives,"* Prentice Hall PTR, 2001.

5. R.Krishnan, *"Electric Motor Drives Modeling, Analysis and Control,"* Prentice Hall of India, 2005.

6. Muhammad H.Rashid, *"Power Electronics Circuits, Devices and Applications,"* Pearson Education, Third Edition, 2005.

7. Pragasen Pillay and Ramu Krishnan, "Modeling, Simulation, and Analysis of Permanent-Magnet Motor Drives, Part I: The Permanent-Magnet Synchronous Motor Drive", *IEEE Trans. on Industry Applications*, Vol.25, No. 2, March/April 1989, PP.265-273.

8. F.M. Abdel-Kader and S.M.Osheba, "Performance Analysis of PMSM Part 1: Dynamic Performance," *IEEE Trans. on Energy Conversions*, Vol. 5, No. 2, June 1990, pp.366-373.

9. Chuen Chien Lee, "Fuzzy Logic in Control Systems: Fuzzy Logic Controller - Part I," *IEEE Trans. on Systems, Man and Cybernetics*, Vol.20, No.2, March/April 1990, pp.404-418.

10. Chuen Chien Lee, "Fuzzy Logic in Control Systems: Fuzzy Logic Controller - Part II," *IEEE Trans. on Systems, Man and Cybernetics*, Vol.20, No.2, March/April 1990, pp.419-435.

11. Pragasen Pillay and Ramukrishnan, "Application Characteristics of Permanent Magnet Synchronous and Brushless DC Motors for Servo Drives," *IEEE Trans. on Industry Applications*, Vol.21, No.5, September/October 1991, pp.986-996.

12. Alfio Consoli and Angelo Raciti, "Analysis of Permanent Magnet Synchronous Motors," *IEEE Trans. on Industry Applications*, Vol.27, No. 2, March/April 1991, PP.350-354.

13. Rusong Wu and Gordon R.slemon, "A Permanent Magnet Motor Drive without a Shaft Sensor," *IEEE Trans. on Industry Applications*, Vol.27, No.5, September/October 1991, pp.1005-1011.

14. Thomas M.Jahns, "Motion control with Permanent-Magnet AC Machines," *in Proc., 1994, IEEE*, Vol.82, No.8, pp.1241-1252.

15. Bhim Singh, C.L.Putta Swamy, B.P.Singh, A.Chandra and K.Al-haddad, "Performance Analysis of Fuzzy Logic Controlled Permanent Magnet Synchronous Motor Drive," *in Proc., 1995 IEEE IECON 21$^{st}$ International Conf. on Industrial Electronics, Control and Instrumentation*, Vol.1, pp.399-405.

16. Hoang Le – Huy, "An Adaptive Fuzzy Controller for Permanent Magnet AC Servo Drives," *in proc., 1995 Industry Application Conf.*, Vol.1, pp.104-110.

17. Tomonobu Senjyu, Tsuyoshi Shimabukuro and Katsumi Uezato, "Vector Control of Permanent Magnet Synchronous Motors without Position and Speed Sensors," *in proc., 1995, 26$^{th}$ Annual IEEE Power Electronic Specialists Conf. (PESC)*, Vol.2, pp.759-765.

18. Sanjiv Kumar, Bhim Singh and J.K.Chatterjee, "Hybrid Speed Controller for Vector Controlled Cage Induction Motor Drive," *in proc., 1998 International Conf. on Power Electronic Drives and Energy Systems for Industrial Growth*, Vol.1, pp.147-152.

19. Jun Hu and Bin Wu, "New Integration Algorithms for Estimating Motor Flux over a Wide Speed Range," *IEEE Trans. on Power Electronics*, Vol.13, No.5, September 1998, pp.969-977.

20. Driss Yousti, Mohammed Azizi and Abdallah Saad, "A New Position and Speed Estimation Technique for PMSM with Drift Correction of the Flux Linkage," *in proc., 2001, Power System Components and Systems*, vol.29, pp.597-613.

21. Bhim Singh and Sumith Ghatak Choudhuri. "Fuzzy Logic Based Speed Controllers for Vector Controlled Induction Motor Drive," *in proc., 2002, IETE Journal*, Vol.48, No.6, pp 441-447.

22. Amar Nath Tiwari, "Investigations on Permanent Magnet Synchronous Motor Drive," Ph.d. thesis, IIT-Roorkee, August 2003.

23. N.Senthil Kumar, K.Saravanan, "Speed Control of PMSM Drive Using VSI," *in proc., 2004, The 30th Annual Conf. of the IEEE Industrial Electronics Society,* November 2 - 6, Busan, Korea, pp.888-895.

24. Bhim Singh, B.P.Singh and S.Dwivedi, "A State of Art on Different Configurations of Permanent Magnet Brushless Machines," *in proc., 2006, IE(I) Journal,* Vol.87, pp.63-73.

25. Bhim Singh, B.P.Singh and Sanjeet Dwivedi, "DSP Based Implementation of Hybrid Fuzzy PI speed Controller Permanent Magnet Synchronous Motor Drive," *in proc., 2007, International Journal of Emerging Electric Power Systems,* Vol.8, Issue 2, pp.1-22.

26. User Manual of I-8438/8838 Embedded Controller.

# Appendix- A

## Specifications of simulated motor parameters

---

### 1. Permanent Magnet Synchronous Motor 1:

| | |
|---|---|
| Power Rating | 1.1 kw |
| Rated Torque (Tr) | 3.5 N-m |
| Phase Resistance (Rs) | 2.875 $\Omega$ |
| Phase Inductance (Ls) | 8.5 e-3 H |
| Flux Induced by Magnets ($\lambda$) | 0.175 Wb |
| Moment of Inertia (J) | 0.8 e-3 Kg-m$^2$ |
| No. of Pole Pairs (P) | 4 |

### 2. Permanent Magnet Synchronous Motor 2:

| | |
|---|---|
| Power Rating | 3.5 kw |
| Rated Torque (Tr) | 11 N-m |
| Phase Resistance (Rs) | 0.2 $\Omega$ |
| Phase Inductance (Ls) | 8.5 e-3 H |
| Flux Induced by Magnets ($\lambda$) | 0.175 Wb |
| Moment of Inertia (J) | 0.089 Kg-m$^2$ |
| Friction Constant (F) | 0.005 N-m-s |
| No. of Pole Pairs (P) | 4 |

## Appendix- B

## Specifications of controller parameters

**Permanent Magnet Synchronous Motor 1:**

| | |
|---|---|
| PI controller | : $K_p = 0.55$, $K_i = 0.5$ |
| Fuzzy Controller | : $K_1 = 0.004$, $K_2 = 0.001$, $K_3 = 150$ |
| Hybrid Controller | : $K_p = 0.55$, $K_i = 0.8$, $K_1 = 0.004$, $K_2 = 0.001$, $K_3 = 150$ |
| FPPI Controller | : $K_p = 0.55$, $K_i = 0.5$, $K_1 = 0.004$, $K_2 = 0.001$, $K_3 = 150$ |

**Permanent Magnet Synchronous Motor 2:**

| | |
|---|---|
| PI controller | : $K_p = 3.2$, $K_i = 0.022$ |
| Fuzzy Controller | : $K_1 = 0.003$, $K_2 = 0.00001$, $K_3 = 1500$ |
| Hybrid Controller | : $K_p = 2.3$, $K_i = 0.025$, $K_1 = 0.003$, $K_2 = 0.00001$, $K_3 = 1500$ |
| FPPI Controller | : $K_p = 1.5$, $K_i = 0.025$, $K_1 = 0.003$, $K_2 = 0.00001$, $K_3 = 1500$ |

# Appendix- C

## Hardware Specifications for I-8438/8838

**General environment:**

Operating temperature: -25 C to +75 C

Storage temperature: -30 C to +85 C

Humidity: 5 ~ 95%

Built-in power protection & network protection circuit

**System:**

CPU: RDC, 80MHz, or compatible

SRAM: 512K bytes

FLASH ROM: 512K bytes

**COM ports for the I-8438 & 8838:**

COM1=RS-232, COM3=RS232/RS485, COM4=RS-232

Ethernet: 10 BaseT

RTC, NVRAM & EEPROM

Program downloads from COM1 & Ethernet

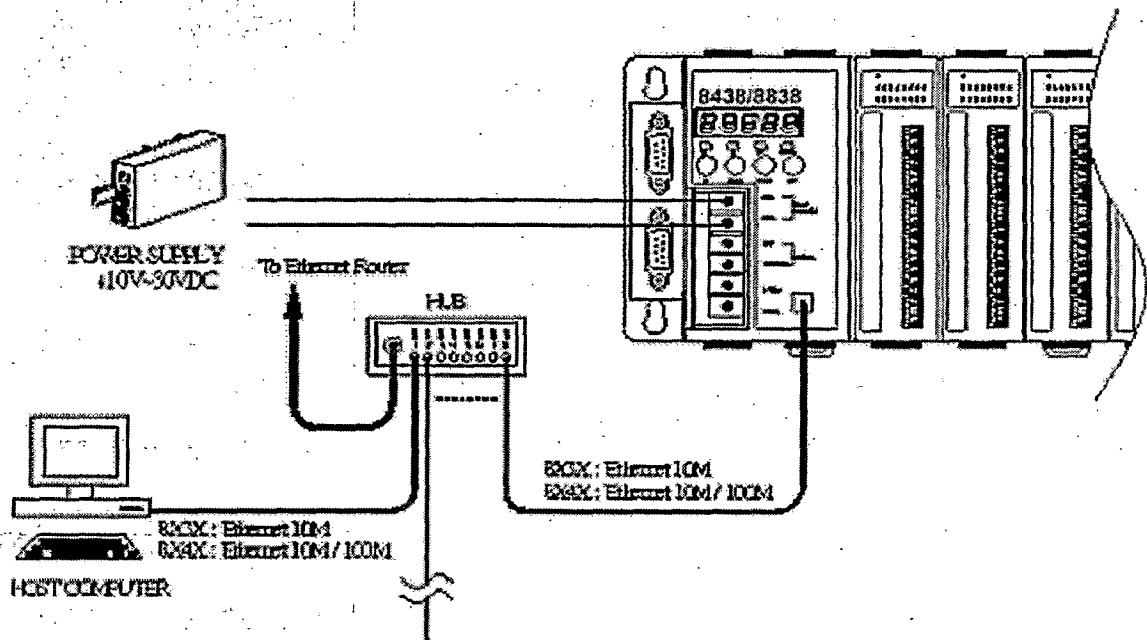Built-in 64-bit hardware unique serial number

Built-in Watchdog Timer

I/O Expansion Slot

4-slot for I-8438

8-slot for I-8838

# Appendix- D

## Hardware Connection of I-8438/8838



1. Connect the network cable to the RJ-45 connector and a hub.

2. Apply power (+Vs, GND) to I-8438/8838. The DC power can be the value from +10V to +30V.

3. Check the 5 digits of the 7-segment LED. If the firmware is running, the IP address of the I-8438/8838 will be displayed.